REFERENCES

1. **Arnaudeau S, Frieden M, Nakamura K, Castelbou C, Michalak M, and Demaurex N.** Calreticulin differentially modulates calcium uptake and release in the endoplasmic reticulum and mitochondria. *J Biol Chem* 277: 46696–46705, 2002.
2. **Bastianutto C, Clementi E, Codazzi F, Podini P, De Giorgi F, Rizzuto R, Meldolesi J, and Pozzan T.** Overexpression of calreticulin increases the Ca^{2+} capacity of rapidly exchanging Ca^{2+} stores and reveals aspects of their lumenal microenvironment and function. *J Cell Biol* 130: 847–855, 1995.
3. **Berridge MJ, Bootman MD, and Lipp P.** Calcium: a life and death signal. *Nature* 395: 645–648, 1998.
4. **Bishopric NH, Andreka P, Slepak T, and Webster KA.** Molecular mechanisms of apoptosis in the cardiac myocyte. *Curr Opin Pharmacol* 1: 141–150, 2001.
5. **Buckler KJ and Vaughan-Jones RD.** Effects of mitochondrial uncouplers on intracellular calcium, pH and membrane potential in rat carotid body type I cell. *J Physiol* 513: 819–833, 1998.
6. **Chen Q, Jones TW, and Stevens JL.** Early cellular events couple covalent binding of reactive metabolites to cell killing by nephrotoxic cysteine conjugates. *J Cell Physiol* 161: 293–302, 1994.
6a.**Curran-Everett D and Benos DJ.** Guidelines for reporting statistics in journals published by the American Physiological Society. *Am J Physiol Cell Physiol* 287: 243–245, 2004.
7. **Ermak G and Davies KJA.** Calcium and oxidative stress: from cell signaling to cell death. *Mol Immunol* 38: 713–721, 2001.
8. **Fasolato C, Pizzo P, and Pozzan T.** Delayed activation of the store-operated calcium current induced by calreticulin overexpression in RBL-1 cells. *Mol Biol Cell* 9: 1513–1522, 1998.
9. **Fisher SA, Langille BL, and Srivastava D.** Apoptosis during cardiovascular development. *Circ Res* 87: 856–864, 2000.
10. **Gafni J, Munsch JA, Lam TH, Catlin MC, Costa LG, Molinski TF, and Pessah IN.** Xestospongins: potent membrane permeable blockers of the inositol 1,4,5-trisphosphate receptor. *Neuron* 19: 723–733, 1997.
11. **Gavrieli Y, Sherman Y, and Ben-Sasson SA.** Identification of programmed cell death in situ via specific labeling of nuclear DNA fragmentation. *J Cell Biol* 119: 493–501, 1992.
12. **Gill C, Mestril R, and Samali A.** Losing heart: the role of apoptosis in heart disease—a novel therapeutic target? *FASEB J* 16: 135–146, 2002.
13. **Glading A, Chang P, Lauffenburger DA, and Wells A.** Epidermal growth factor receptor activation of calpain is required for fibroblast motility and occurs via an ERK/MAP kinase signaling pathway. *J Biol Chem* 275: 2390–2398, 2000.
14. **Grover AK and Samson SE.** Effect of superoxide radical on Ca^{2+} pumps of coronary artery. *Am J Physiol Cell Physiol* 255: C297–C303, 1988.
15. **Grover AK, Samson SE, and Fomin VP.** Peroxide inactivates calcium pumps in pig coronary artery. *Am J Physiol Heart Circ Physiol* 263: H537–H543, 1992.
16. **Grynkiewicz G, Poenie M, and Tsien RY.** A new generation of Ca^{2+} indicators with greatly improved fluorescence properties. *J Biol Chem* 260: 3440–3450, 1985.
17. **Holaska JM, Black BE, Love DC, Hanover JA, Leszyk J, and Paschal BM.** Calreticulin is a receptor for nuclear export. *J Cell Biol* 152: 127–140, 2001.
18. **Hung CC, Ichimura T, Stevens JL, and Bonventre JV.** Protection of renal epithelial cells against oxidative injury by endoplasmic reticulum stress preconditioning is mediated by ERK1/2 activation. *J Biol Chem* 278: 29317–29326, 2003.
19. **Ihara Y, Sakamoto Y, Mihara M, Shimizu K, and Taniguchi N.** Overexpression of N-acetylglucosaminyltransferase III disrupts the tyrosine phosphorylation of Trk with resultant signaling dysfunction in PC12 cells treated with nerve growth factor. *J Biol Chem* 272: 9629–9634, 1997.
20. **Ihara Y, Kageyama K, and Kondo T.** Overexpression of calreticulin sensitizes SERCA2a to oxidative stress. *Biochem Biophys Res Commun* 329: 1343–1349, 2005.
21. **Imanaka-Yoshida K, Amitani A, Ioshii SO, Koyabu S, Yamakado T, and Yoshida T.** Alteration of expression and distribution of the Ca^{2+}-sorting proteins in endo/sarcoplasmic reticulum during differentiation of rat cardiomyocytes. *J Mol Cell Cardiol* 28: 553–562, 1996.
22. **John LM, Lechleiter JD, and Camacho P.** Differential modulation of SERCA2 isoforms by calreticulin. *J Cell Biol* 142: 963–973, 1998.
23. **Johnson S, Michalak M, Opas M, and Eggleton P.** The ins and outs of calreticulin: from the ER lumen to the extracellular space. *Trends Cell Biol* 11: 122–129, 2001.
24. **Kageyama K, Ihara Y, Goto S, Urata Y, Toda G, Yano K, and Kondo T.** Overexpression of calreticulin modulates protein kinase B/Akt signaling to promote apoptosis during cardiac differentiation of cardiomyoblast H9c2 cells. *J Biol Chem* 277: 19255–19264, 2002.
25. **Kaufman RJ.** Orchestrating the unfolded protein response in health and disease. *J Clin Invest* 110: 1389–1398, 2002.
26. **Kimura J, Miyamae S, and Noma A.** Identification of sodium-calcium exchange current in single ventricular cells of guinea-pig. *J Physiol* 384: 199–222, 1987.
27. **Kurebayashi N and Ogawa Y.** Depletion of Ca^{2+} in the sarcoplasmic reticulum stimulates Ca^{2+} entry into mouse skeletal muscle fibres. *J Physiol* 533: 185–199, 2001.
28. **Liu H, Bowes RC III, van de Water B, Sillence C, Nagelkerke JF, and Stevens JL.** Endoplasmic reticulum chaperones GRP78 and calreticulin prevent oxidative stress, Ca^{2+} disturbances, and cell death in renal epithelial cells. *J Biol Chem* 272: 21751–21759, 1997.
29. **Liu H, Miller E, van de Water B, and Stevens JL.** Endoplasmic reticulum stress proteins block oxidant-induced Ca^{2+} increases and cell death. *J Biol Chem* 273: 12858–12862, 1998.
30. **Lounsbury KM, Hu Q, and Ziegelstein RC.** Calcium signaling and oxidant stress in the vasculature. *Free Radic Biol Med* 28: 1362–1369, 2000.
31. **McConkey DJ and Orrenius S.** The role of calcium in the regulation of apoptosis. *Biochem Biophys Res Commun* 239: 357–366, 1997.
32. **Mery L, Mesaeli N, Michalak M, Opas M, Lew DP, and Krause KH.** Overexpression of calreticulin increases intracellular Ca^{2+} storage and decreases store-operated Ca^{2+} influx. *J Biol Chem* 271: 9332–9339, 1996.
33. **Mesaeli N, Nakamura K, Zvaritch E, Dickie P, Dziak E, Krause KH, Opas M, MacLennan DH, and Michalak M.** Calreticulin is essential for cardiac development. *J Cell Biol* 144: 857–868, 1999.
34. **Mesaeli N and Phillipson C.** Impaired p53 expression, function, and nuclear localization in calreticulin-deficient cells. *Mol Biol Cell* 15: 1862–1870, 2004.
35. **Michalak M, Corbett EF, Mesaeli N, Nakamura K, and Opas M.** Calreticulin: one protein, one gene, many functions. *Biochem J* 344: 281–292, 1999.
36. **Morgan-Boyd R, Stewart JM, Vavrek RJ, and Hassid A.** Effects of bradykinin and angiotensin II on intracellular Ca^{2+} dynamics in endothelial cells. *Am J Physiol Cell Physiol* 253: C588–C598, 1987.
37. **Morishima N, Nakanishi K, Takenouchi H, Shibata T, and Yasuhiko Y.** An endoplasmic reticulum stress-specific caspase cascade in apoptosis: cytochrome c-independent activation of caspase-9 by caspase-12. *J Biol Chem* 277: 34287–34294, 2002.
38. **Mosmann T.** Rapid colorimetric assay for cellular growth and survival: application to proliferation and cytotoxicity assays. *J Immunol Methods* 65: 55–63, 1983.
39. **Murata H, Ihara Y, Nakamura H, Yodoi J, Sumikawa K, and Kondo T.** Glutaredoxin exerts antiapoptotic effect by regulating redox state of Akt. *J Biol Chem* 278: 50226–50233, 2003.
40. **Nakagawa T and Yuan J.** Cross-talk between two cysteine proteases: activation of caspase-12 by calpain in apoptosis. *J Cell Biol* 150: 887–894, 2000.
41. **Nakamura K, Bossy-Wetzel E, Burns K, Fadel MP, Lozyk M, Goping IS, Opas M, Bleackley RC, Green DR, and Michalak M.** Changes in endoplasmic reticulum luminal environment affect cell sensitivity to apoptosis. *J Cell Biol* 150: 731–740, 2000.
42. **Nakamura K, Robertson M, Liu G, Dickie P, Nakamura K, Guo JQ, Duff HJ, Opas M, Kavanagh K, and Michalak M.** Complete heart block and sudden death in mice overexpressing calreticulin. *J Clin Invest* 107: 1245–1253, 2001.
43. **Pinton P, Ferrari D, Rapizzi E, Di Virgilio F, Pozzan T, and Rizzuto R.** The Ca^{2+} concentration of the endoplasmic reticulum is a key deter-

minant of ceramide-induced apoptosis: significance for the molecular mechanism of Bcl-2 action. *EMBO J* 20: 2690–2701, 2001.

44. Rao RV, Ellerby HM, and Bredesen DE. Coupling endoplasmic reticulum stress to the cell death program. *Cell Death Differ* 11: 372–380, 2004.

45. Rauch F, Prud'homme J, Arabian A, Dedhar S, and St-Arnaud R. Heart, brain, and body wall defects in mice lacking calreticulin. *Exp Cell Res* 256: 105–111, 2000.

46. Roderick HL, Llewellyn DH, Campbell AK, and Kendall JM. Role of calreticulin in regulating intracellular Ca^{2+} storage and capacitative Ca^{2+} entry in HeLa cells. *Cell Calcium* 24: 253–262, 1998.

47. Sauer H, Rahimi G, Hescheler J, and Wartenberg M. Role of reactive oxygen species and phosphatidylinositol 3-kinase in cardiomyocyte differentiation of embryonic stem cells. *FEBS Lett* 476: 218–223, 2000.

48. Scorrano L, Oakes SA, Opferman JT, Cheng EH, Sorcinelli MD, Pozzan T, and Korsmeyer SJ. BAX and BAK regulation of endoplasmic reticulum Ca^{2+}: a control point for apoptosis. *Science* 300: 135–139, 2003.

49. Sumida M and Tonomura Y. Reaction mechanism of the Ca^{2+}-dependent ATPase of sarcoplasmic reticulum from the skeletal muscle: X. Direct evidence for Ca^{2+} translocation coupled with formation of a phosphorylated intermediate. *J Biochem (Tokyo)* 75: 283–297, 1974.

50. Thastrup O, Cullen PJ, Drøbak BK, Hanley MR, and Dawson AP. Thapsigargin, a tumor promoter, discharges intracellular Ca^{2+} stores by specific inhibition of the endoplasmic reticulum Ca^{2+}-ATPase. *Proc Natl Acad Sci USA* 87: 2466–2470, 1990.

51. Tsutsui H, Ishibashi Y, Imanaka-Yoshida K, Yamamoto S, Yoshida T, Sugimachi M, Urabe Y, and Takeshita A. Alteration in sarcoplasmic reticulum calcium-storing proteins in pressure-overload cardiac hypertrophy. *Am J Physiol Heart Circ Physiol* 272: H168–H175, 1997.

52. Turner NA, Xia F, Azhar G, Zhang X, Liu L, and Wei JY. Oxidative stress induces DNA fragmentation and caspase activation via the c-Jun NH_2-terminal kinase pathway in H9c2 cardiac muscle cells. *J Mol Cell Cardiol* 30: 1789–1801, 1998.

53. Xu K, Tavernarakis N, and Driscoll M. Necrotic cell death in *C. elegans* requires the function of calreticulin and regulators of Ca^{2+} release from the endoplasmic reticulum. *Neuron* 31: 957–971, 2001.

54. Xu W, Longo FJ, Wintermantel MR, Jiang X, Clark RA, and DeLisle S. Calreticulin modulates capacitative Ca^{2+} influx by controlling the extent of inositol 1,4,5-triphosphate-induced Ca^{2+} store depletion. *J Biol Chem* 275: 36676–36682, 2000.

55. Yang F, He XP, Russell J, and Lu B. Ca^{2+} influx-independent synaptic potentiation mediated by mitochondrial Na^{+}-Ca^{2+} exchanger and protein kinase C. *J Cell Biol* 163: 511–523, 2003.

56. Yasuoka C, Ihara Y, Ikeda S, Miyahara Y, Kondo T, and Kohno S. Antiapoptotic activity of Akt is down-regulated by Ca^{2+} in myocardiac H9c2 cells: evidence of Ca^{2+}-dependent regulation of protein phosphatase 2Ac. *J Biol Chem* 279: 51182–51192, 2004.

57. Zhang L, Song L, and Parker EM. Calpain inhibitor I increases β-amyloid peptide production by inhibiting the degradation of the substrate of γ-secretase: evidence that substrate availability limits β-amyloid peptide production. *J Biol Chem* 274: 8966–8972, 1999.

17β-Estradiol Protects against Oxidative Stress-induced Cell Death through the Glutathione/Glutaredoxin-dependent Redox Regulation of Akt in Myocardiac H9c2 Cells*

Yoshishige Urata[‡1,2], Yoshito Ihara[‡1], Hiroaki Murata[‡], Shinji Goto[‡], Takehiko Koji[§], Junji Yodoi[¶], Satoshi Inoue[‖], and Takahito Kondo[‡]

From the ‡Department of Biochemistry and Molecular Biology in Disease, Atomic Bomb Disease Institute, Nagasaki University Graduate School of Biomedical Sciences, 1-12-4 Sakamoto, Nagasaki 852-8523, Japan, the §Department of Histology and Cell Biology, Nagasaki University Graduate School of Biomedical Sciences, 1-12-4 Sakamoto, Nagasaki 852-8523, Japan, the ¶Department of Biological Responses, Institute for Viral Research, Graduate School of Medicine, Kyoto University, 53 Shogoin, Kawahara-cho, Sakyo-ku, Kyoto 606-8397, Japan, and the ‖Department of Geriatric Medicine, Graduate School of Medicine, University of Tokyo, 7-3-1 Hongo, Bunkyo-ku, Tokyo 113-8655, Japan

The GSH/glutaredoxin (GRX) system is involved in the redox regulation of certain enzyme activities, and this system protects cells from H_2O_2-induced apoptosis by regulating the redox state of Akt (Murata, H., Ihara, Y., Nakamura, H., Yodoi, J., Sumikawa, K., and Kondo, T. (2003) *J. Biol. Chem.* 278, 50226–50233). Estrogens, such as 17β-estradiol (E_2), play an important role in development, growth, and differentiation and appear to have protective effects on oxidative stress mediated by estrogen receptor α (ERα). However, the role of the ERβ-mediated pathway in this cytoprotection and the involvement of E_2 in the redox regulation are not well understood. In the present study, we demonstrated that E_2 protected cardiac H9c2 cells, expressing ERβ from H_2O_2-induced apoptosis concomitant with an increase in the activity of Akt. E_2 induced the expression of glutaredoxin (GRX) as well as γ-glutamylcysteine synthetase, a rate-limiting enzyme for the synthesis of GSH. Inhibitors for both γ-glutamylcysteine synthetase and GRX and ICI182,780, a specific inhibitor of ERs, abolished the protective effect of E_2 on cell survival as well as the activity of Akt, suggesting that ERβ is involved in the cytoprotection and redox regulation by E_2. Transcription of the GRX gene was enhanced by E_2. The promoter activity of GRX was up-regulated by an ERβ-dependent element. These results suggest that the GRX/GSH system is involved in the cytoprotective and genomic effects of E_2 on the redox state of Akt, a pathway that is mediated, at least in part, by ERβ. This mechanism may also play an antiapoptotic role in cancer cells during carcinogenesis or chemotherapy.

Oxidative stress is a principle cause of the development of aging and diseases such as inflammation, infection, cancer, and cardiovascular disorders (1, 2). Exogenous or endogenous sources of oxidative stress and weakened antioxidative defenses can damage macromolecules such as DNA, lipids, and proteins.

Estrogens play an important role in development, growth, and the differentiation of both female and male secondary sex characteristics (3). Protective effects of estrogen, such as 17β-estradiol (E_2),[3] on oxidative stress have been indicated (4). E_2 regulates longevity signals to enhance resistance to oxidative stress in mice. Inhibitory effects of E_2 on atherosclerosis are mediated by COX-2-derived prostacyclin (5). E_2 induces production of antioxidative enzymes, such as superoxide dismutase (6), γ-glutamylcysteine synthetase (γ-GCS), and glutathione S-transferase (7). The effects of E_2 are mediated mostly through ERα, which functions as a ligand-induced transcription factor and belongs to the nuclear receptor superfamily (8). ERα binds to a variety of ligands and displays tissue-specific effects through estrogen-response element (ERE). When estrogen-responsive genes do not contain EREs, ERα can up-regulate gene expression through AP-1 and Sp1 sites (9). Another ER, ERβ, is expressed in cells targeted by E_2, including cardiomyocytes (10). However, the role of ERβ in protection against oxidative stress has not been well studied.

Protein thiols act as redox-sensitive switches and are believed to be a key element in maintaining the cellular redox balance. The redox state of protein thiols is regulated by oxidative stress and redox signaling and important to cellular functions. To maintain the cellular thiol-disulfide redox status, living cells possess two major systems, the thioredoxin (TRX)/TRX reductase system and the glutathione (γ-glutamylcysteinyl glycine, GSH)/glutaredoxin (GRX) system (11). GSH is synthesized in two sequential enzymatic reactions that are each catalyzed by a rate-limiting enzyme, γ-GCS, and GSH synthetase (12). GRX, also known as thioltransferase, was first discovered as a GSH-dependent hydrogen donor for ribonucleotide reductase in *Escherichia coli* mutants lacking TRX (13). Oxidized GRX is recycled to the reduced form by GSH with the formation of glutathione disulfide and regeneration of GSH by coupling with NADPH and glutathione disulfide reductase (14). GRX functions via a disulfide exchange reaction by utilizing the active site, Cys-Pro-Tyr-Cys, which specifically and efficiently catalyzes the reduction

[3] The abbreviations used are: E_2, 17β-estradiol; ER, estrogen receptor; ERE, estrogen-response element; GRX, glutaredoxin; γ-GCS, γ-glutamylcysteine synthetase; PP2A, protein phosphatase 2A; MTT, 3-(4,5-dimethyl-thiazole-2-yl)-2,5-diphenyltetrazolium bromide; HRP, horseradish peroxidase; PPT, propylpyrazoletriol; TBS, Tris-buffered saline; PDK1, 3-phosphoinositide-dependent protein kinase-1; TRX, thioredoxin; AMS, 4-acetamido-4'-maleimidylstilbene-2,2'-disulfonic acid; PBS, phosphate-buffered saline; RT, reverse transcription; BSO, buthionine sulfoximine; EpRE, electrophoretic response element.

of protein-SSG mixed disulfide (15). GRX also partially shares its function as a redox sensor with TRX (16, 17). Recently, we have found that GRX protects against oxidative stress-induced cell death from apoptosis by regulating the redox state of Akt (18).

Akt/protein kinase B is a pleckstrin homology domain-containing serine/threonine kinase and a critical component of an intracellular signaling pathway that exerts effects on survival and apoptosis (19). Akt has been found to be responsive to extracellular signaling factors, oxidative and osmotic stress, irradiation, and ischemic stress (20). Akt can phosphorylate Bad, caspase-9, and forkhead-related transcription factors, leading to an inhibition of apoptosis (21). The unphosphorylated form of Akt is virtually inactive, and phosphorylation at Thr^{308} and Ser^{473} stimulates its activity. Inactivation of Akt also occurs via dephosphorylation of the two phosphorylation sites by protein phosphatase 2A (PP2A) (22, 23). The activation of Akt contributes to the survival of H_2O_2-treated cells (24).

It has been reported that the function of ER-mediated transcriptional activity is regulated by redox (25). However, the precise mechanisms of redox regulation in the E_2-mediated signal pathways have not been clarified. Here we describe a mechanism for the antiapoptotic effect of E_2 through the regulation of the redox state of Akt under oxidative stress. Treatment of cardiac H9c2 cells with E_2 for 18 h protected against H_2O_2-induced apoptosis. E_2 induced the expression of GRX and γ-GCS, at least in part, through ERβ-mediated regulation. Elevated GSH and GRX levels potentiated the redox of Akt on the exposure of cells to H_2O_2.

MATERIALS AND METHODS

Reagents—Anti-PP2A scaffolding A subunit (PR65) antibody was obtained from Santa Cruz Biotechnology. Antibodies against human ERα (clone ER88) and ERβ (polyclonal) were from Kyowa Medex (Tokyo, Japan). Horseradish peroxidase (HRP)-conjugated goat anti-rabbit IgG F was purchased from MBL (Nagoya, Japan). HRP-goat anti-mouse IgG F was from Chemicon International (Temocula, CA). Normal goat IgG, normal rabbit IgG, and normal mouse IgG were from Sigma. Anti-Akt and anti-phospho-(Ser^{473})-Akt antibodies were from Cell Signaling Technology. Anti-PP2A catalytic C subunit antibody was from BD Transduction Laboratories. 3-(4,5-dimethyl-thiazol-2-yl)-2,5-diphenyltetrazolium bromide (MTT) was from Sigma. 4-Acetamido-4'-maleimidylstilbene-2,2'-disulfonic acid (AMS) was purchased from Molecular Probes, Inc. (Eugene, OR). H_2O_2 and $CdCl_2$ were from Wako Pure Chemicals (Osaka, Japan). ICI182,780 and propylpyrazoletriol (PPT) were from Tocris (Ballwin, MO).

Cell Culture—H9c2 cells, a clonal line derived from embryonic rat heart, and human breast cancer SK-BR-3 (SKB3) cells, and MDA-MB-231 (MDA) cells, were obtained from the American Type Culture Collection (CRL-1446). Human breast cancer MCF7 cells were from The Cell Resource Center for Biomedical Research Institute of Development, Aging, and Cancer, Tohoku University (Sendai, Japan). H9c2 cells were routinely maintained in Dulbecco's modified Eagle's medium, or MDA and SKB3 cells were maintained in RPMI1640 medium. The cells were supplied with 10% fetal calf serum in a humidified atmosphere of 95% air and 5% CO_2 at 37 °C (23).

Cell Viability—Cell viability was determined by a MTT assay as described (26). Briefly, cells (1500–5000) were placed in 100 μl of medium per well in 96-well plates. Four hours after treatment with various concentrations of H_2O_2, the cells were incubated for 4 h at 37 °C with 3-(4,5-dimethylthiazol-e-yl)-2,5-diphenyltetrazolium bromide (652 μg/ml) and lysed with 100 μl of 20% SDS, 50% N,N-dimethylformamide (pH 4.7) in each well. After an overnight incubation at 37 °C, the absorbance at 570 nm was measured. Wells without cells served as blanks.

Nuclear Condensation—For the histochemical analysis, cells were maintained in a four-well Lab Tec Chamber (Nalge Nunc International, Naperville, IL). After treatment with H_2O_2, cells were treated with 10 μM Hoechst 33342 for 30 min to estimate the extent of nuclear condensation. They were then washed again with PBS. Fluorescence intensity was examined using an Axioskop2 fluorescence microscope (Carl Zeiss, Jena, Germany), and the findings were analyzed using a charge-coupled device camera (Axio-Cam) and AxioVision software.

Morphological Staining—The immunohistochemical analysis to examine the expression of ERα and ERβ was performed as described previously (27). Briefly, cells were fixed with 4% paraformaldehyde in PBS and then preincubated with blocking solution for 1 h at room temperature. For ERβ 10% normal goat serum and 1% bovine serum albumin in PBS and for ERα 500 μg/ml of normal goat IgG and 1% bovine serum albumin in PBS were used, respectively. Next, the samples were incubated with the primary antibodies overnight and washed three times with 0.075% Brij 35 in PBS. Then samples were reacted with HRP-goat anti-mouse IgG or HRP-goat anti-rabbit IgG for 1 h at room temperature and washed three times with 0.075% Brij 35 in PBS. HRP sites were visualized with H_2O_2 and DAB solution or H_2O_2 and DAB in the presence of nickel and cobalt ions. As a negative control, normal rabbit IgG and normal mouse IgG were used instead of the primary antibodies. The results of immunohistochemistry for ERs were graded as positive or negative, compared with the staining with IgG or serum of a normal rabbit or mouse.

Immunoblot Analysis—Cultured cells were harvested and lysed for 20 min at 4 °C in lysis buffer as described previously (17). The supernatants obtained by centrifugation of the lysates at 8000 × g for 15 min were used in subsequent experiments. Protein concentrations were determined using a BCA assay kit (Pierce). Protein samples were electrophoresed on 10, 12.5, or 15% SDS-polyacrylamide gels under reducing conditions, except for thiol-modified protein samples. The proteins in the gels were transferred onto nitrocellulose membranes. The membranes were blocked in Tris-buffered saline (10 mM Tris-HCl (pH 7.5) and 0.15 M NaCl; TBS) containing 0.05% Tween 20 (v/v) (TBST) and 5% (w/v) nonfat dry milk and then reacted with primary antibodies in TBST containing 3% (w/v) bovine serum albumin overnight with constant agitation at 4 °C. After several washes with TBST, the membranes were incubated with horseradish peroxidase-conjugated anti-IgG antibodies. Proteins in the membranes were then visualized using the enhanced chemiluminescence detection kit (Amersham Biosciences) according to the manufacturer's instructions.

Akt Activity Assay—Akt activity was assayed using an Akt assay kit (Cell Signaling Technology) according to the manufacturer's directions with GSK3α/β fusion protein (GSK3α/β) as a substrate. Phosphorylation of GSK3α/β was assessed by immunoblot analysis using a specific antibody. Briefly, Akt was immunoprecipitated from cell lysates using the anti-Akt antibody, and then the immunoprecipitates were incubated at 30 °C for 30 min in an assay mixture containing GSK3α/β. Phosphorylated proteins were separated by 12.5% SDS-PAGE and then transferred to nitrocellulose membranes to detect phosphorylated GSK3α/β using an anti-phosphorylated GSK3α/β antibody.

Protein Phosphatase Assay—PP2A activity was assayed spectrophotometrically using a Ser/Thr phosphatase assay kit 1 (Upstate Biotechnology, Inc.) according to the manufacturer's instructions. The phosphopeptide RKpTIRR and p-nitrophenyl phosphate were used as phosphatase substrates.

Determination of Redox States—The redox states of proteins were assessed by modifying free thiol with AMS (28). Briefly, after incubation with or without H_2O_2, cell lysates or proteins were treated with trichloroacetic acid at a final concentration of 7.5% to denature and precipitate

the proteins as well as to avoid any subsequent redox reactions. The protein precipitates were collected by centrifugation at $12,000 \times g$ for 10 min at 4 °C. The pellets were rinsed in acetone and centrifuged twice and then dissolved in a buffer containing 50 mM Tris-HCl (pH 7.4), 1% SDS, and 15 mM AMS. Proteins were then separated by 10% SDS-PAGE without using any reducing agents and blotted to nitrocellulose membranes. Proteins in the membranes were visualized by immunoblotting as described above.

Northern Blot Analysis—A 764-bp DNA fragment (bp 865–1628) of full-length γ-GCS heavy subunit cDNA was obtained by digestion with PstI (29). The probes were radiolabeled with ^{32}P using a random primer labeling kit (Takara Biomedicals, Shiga, Japan). The isolation of cytoplasmic RNA and Northern blotting were essentially performed as described by Sambrook *et al.* (30). Isolated RNAs (30 μg) were electrophoresed on a 1% agarose gel containing 0.6 M formaldehyde, transferred to a nylon membrane, and then hybridized with ^{32}P-labeled probes. Autoradiographed membranes were analyzed using a BAS5000 bioimage analyzer (Fuji Photo Film). A specific system for the amplification of mRNA was also used: an mRNA-selective PCR kit (Takara-Biomedicals; distributed by BioWhittaker, Europe). It had a total volume of 25 μl, comprising 12.5 μl of 2× buffer II, 5 mM $MgCl_2$, 0.5 μM PE1 and PE2, 1 mM each dNTP, 0.4 units of RNAsin (40 units/μl), 0.5 units of Rtase XL (5 units/μl), and 0.5 units of optimized Taq. As material, 1 μg of total RNA extracted from the cells was used. The 330-bp oligonucleotides for GRX (rat GRX sequence, accession number AF167981) were obtained using as a sense primer 5'-GCA TGG CTC AGG AGT TTG TGA ACT GCA AGA TTC AG-3' and, as an antisense primer, 5'-CCT TTC ATA ACT GCA GAG CTC CAA TCT GCT TCA GC-3'. The 410-bp oligonucleotides for β-actin (rat β-actin sequence, accession number BC063166) were obtained using 5'-GAG CTA TGA GCT GCC TGA CG-3' and 5'-AGC ATT TGC GGT GCA CGA TG-3'. The 410-bp oligonucleotides for β-actin (human β-actin sequence, accession number NM_001101.2) were obtained using 5'-GAG CTA CGA GCT GCC TGA CG-3' and 5'-AGC ATT TGC GGT GCA CGA TG-3'. The 325-β oligonucleotides for ERα (rat ERα sequence, accession number AY280663.1) and 280-bp oligonucleotides for ERβ (rat ERβ sequence, accession number U57439) were obtained using 5'-GCT CTT GAC AAA CCC A-3' and 5'-GCG GCG TTG AAC TCG TAG-3' and 5'-GGC TGA GGA AAG CAC CTG TC-3' and 5'-GCG GCG TTG AAC TCG TAG-3', respectively. Similarly, the sense and antisense primers for the oligonucleotides for human ERα (accession number NM_000125.2) were 5'-GAC TAT GCT TCA GGC TAC C-5' and 5'-GGT TCC TGT CCA AGA GCA AG-3', whereas those for human ERβ (accession number NM_001437.1) were 5'-GTG GTC CAT CGC CAG TTA TC-3' and 5'-GCA CTT CTC TGT CTC CGC AC-3', respectively. The RT-amplification was carried out as follows: 30 min at 50 °C for the reverse transcription, denaturation for 5 min at 95 °C, and then a succession of 23 (35 for ERs) cycles as follows: 30 s at 95 °C, 40 s at 65 °C (55 °C for ERs), and 90 s at 72 °C. Amplification took place after 5 min at 72 °C.

Determination of Cellular Glutathione Levels—Total GSH and GSSG levels were measured using a total glutathione quantification kit (Dojindo Molecular Technologies, Inc.) according to the manufacturer's directions. Briefly, 5,5'-dithiobis-(2-nitrobenzoic acid) and GSH react to generate 2-nitro-5-thiobenzoic acid. The concentration of GSH in the sample solution was determined by measuring absorbance at 412 nm. For quantification of GSSG, cell lysates were treated with 2-vinylpyridine and triethanolamine to block the sulfhydryl residue of GSH. GSSG in the sample solution was reduced to GSH using a reducing mixture containing GSSG reductase and NADPH, and the levels of GSSG were determined photometrically as for GSH.

3-Phosphoinositide-dependent Protein Kinase-1 Activity—3-Phosphoinositide-dependent protein kinase-1 (PDK1) activity was estimated using an assay kit according to the manufacturer's instructions (Upstate Biotechnology). Briefly, recombinant human active PDK1 (Upstate Biotechnology) protein was incubated first with inhibitors for 30 min at 30 °C and then with inactive glucocorticoid-inducible kinase 1 (SGK1) for 30 min at 30 °C. Next, the PDK1-dependent SGK1 kinase activity was estimated by incubating the reaction mixture with glycogen synthase kinase 3 (GSK3) peptide as a substrate for 10 min at 30 °C in the presence of [γ-^{32}P]ATP.

Generation of Luciferase Reporter Constructs—A 2.0-kb fragment of the human GRX gene promoter (−2023 to −22) (31) was amplified by PCR using *Pfu* turbo DNA polymerase (Stratagene). The primers used were as follows: a forward primer (5'-GGA CTG AGT GAG AGG CAG ACA ATA GTC TCC-3') and a reverse primer (5'-CGG GAA GAA TCC TCA GTT GCA GGT ATT GCT TGG-3'). The PCR product was subcloned into pUC18 to obtain pUC18-pro-GRX. PUC18-pro-GRX was digested with HindIII, and the resulting fragment containing the promoter region from −2023 to −22 was inserted into the HindIII site of the reporter vector pGL3-Basic (Stratogene) to give pGL3-pro-GRX. To generate a deleted version of the luciferase reporter construct (pGL3-pro-GRX-del), pGL3-pro-GRX was digested with KpnI and PvuII (Takara Biomedicals). Site-directed mutagenesis for luciferase vectors was performed with pGL3-pro-GRX (−2023 to −22) as a template by using a QuikChange site-directed mutagenesis kit (Stratagene). The oligonucleotides used were as follows: electrophoretic response element (EpRE)-like 1 forward (5'-GCT CCC CCT CCG GGA CTC AGA ATC TGG-3') and EpRE-like 1 reverse (5'-CCA GAT TCT GAG TCC CGG AGG GGG AGC-3'). The nucleotide sequence was confirmed by sequencing with an ALFexpress II system (Amersham Biosciences).

Luciferase Activity Assay—Each vector was introduced into H9c2 cells by using Lipofectamine 2000 (Invitrogen) according to the manufacturer's instructions. After 12 h of transfection, cells were harvested for 24 h and then treated with E_2 (100 nM) or left untreated for 18 h. Then luciferase activity was assayed with cellular extracts by using a dual luciferase reporter assay system (Promega).

Electrophoretic Mobility Shift Assay—The electrophoretic mobility shift assay for the GC box and EpRE-like 1 element was performed as described (32). Briefly, oligonucleotides were annealed to double-stranded oligonucleotides and then labeled with [γ-^{32}P]ATP using T4 polynucleotide kinase. Oligonucleotides specific for the GC box and EpRE-like 1 element were prepared according to the nucleotide sequence of the human GRX promoter region. Oligonucleotides used were as follows: EpRE-like 1 element, 5'-CCC TCC GTG ACT CAG AAT CTG GCT TTC-3'; mutated EpRE-like 1 element, 5'-CCC TCC GGG ACT GTA AGC ACT TTA TGC TTC-3'. Binding reactions were performed in 15 μl of reaction mixture (25 mM Tris, pH 7.0, 6.25 mM $MgCl_2$, 0.5 mM EDTA, 0.5 mM dithiothreitol, 50 mM KCl, and 10% glycerol) containing 10 μg of nuclear extract and 25 ng of labeled oligonucleotide. For the supershift assay, specific antibodies were added to the reaction mixture during the binding reaction for 30 min.

Statistical Analysis—Data were presented as means ± S.D. Differences were examined by using Student's *t* test. A value of $p < 0.05$ was considered significant.

RESULTS

Expression of ERs—The expression of ERs in H9c2 cells was estimated immunohistochemically and genetically. Fig. 1 shows the results of the immunohistochemical analysis. Unlike MCF7 cells, which are known to express both ERα (Fig. 1A) and ERβ (Fig. 1B), H9c2 cells expressed ERβ (Fig. 1F) but not ERα (Fig. 1E). Fig. 1I shows the results of the RT-PCR
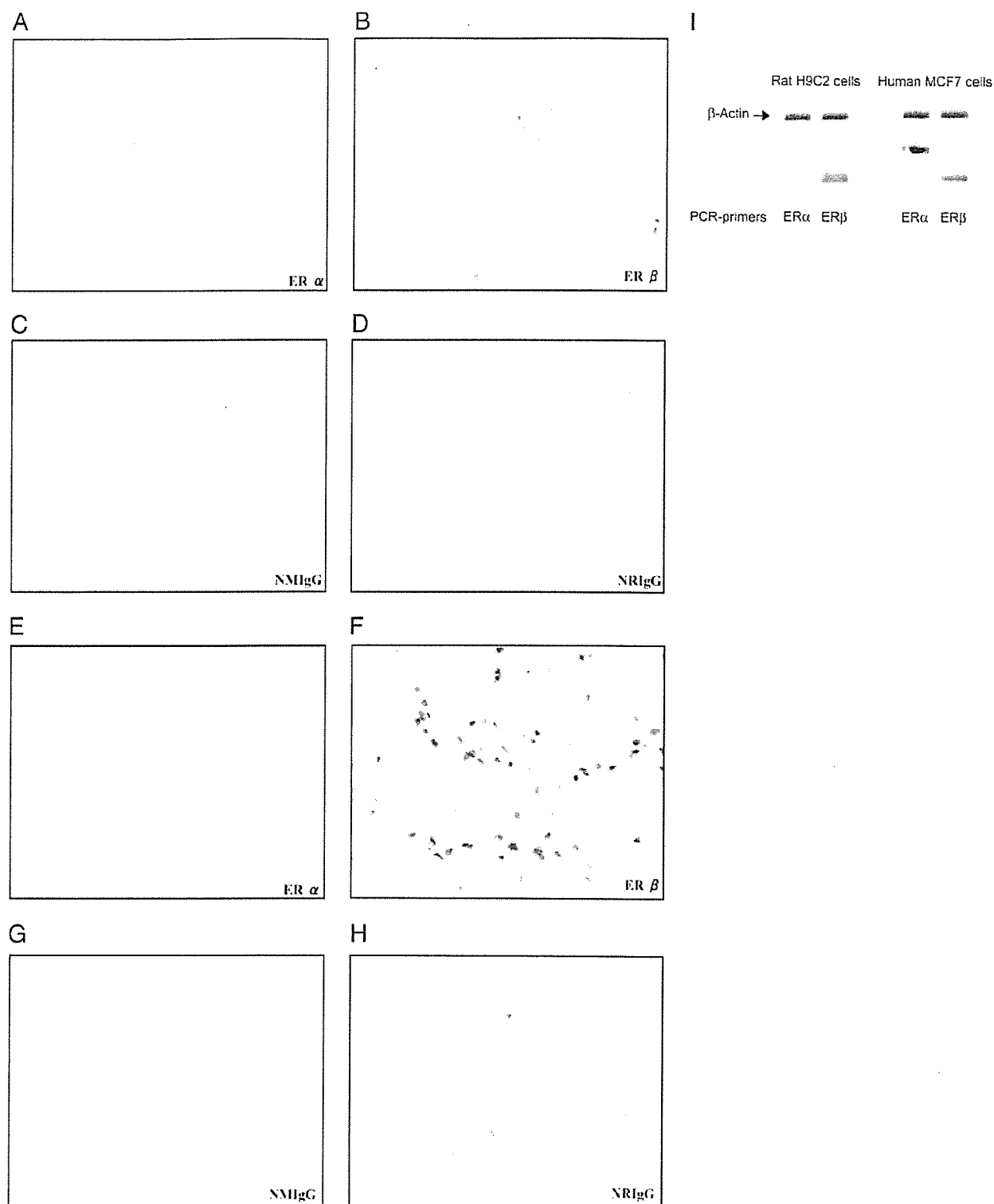
A

ER α

B

ER β

I

	Rat H9C2 cells		Human MCF7 cells	
β-Actin →				
PCR-primers	ERα	ERβ	ERα	ERβ

C

NMIgG

D

NRIgG

E

ER α

F

ER β

G

NMIgG

H

NRIgG

FIGURE 1. **Immunohistochemical analysis for ERs.** The expression of ERs was examined by immunohistochemical analysis. *A–D*, MCF7 cells were treated with antibody against ERα (*A*) and ERβ (*B*). *E–H*, H9c2 cells were treated with antibody against ERα (*E*) and ERβ (*F*). As a negative control, normal mouse IgG (*C* and *G*) or normal rabbit IgG (*D* and *H*) was used. The gene expression of ERs was examined by RT-PCR analysis (*I*) using sense-primers for rat ERα and -β mRNAs in H9c2 cells and those for human mRNA in MCF7 cells.

analysis. ERβ mRNA but not ERα mRNA was detected in H9c2 cells. On the other hand, both ER mRNAs were detected in MCF7 cells.

Cytoprotective Effect of E_2 on Oxidative Stress—We tested the cytoprotective effect of E_2 on oxidative stress-induced apoptosis in H9c2 cells. Hydrogen peroxide induces apoptosis or early mitochondrial dys-

function in cardiac H9c2 cells (32, 33). Since 10% fetal calf serum, required for maintaining cultured cells, reduces oxidative stress modification of cells, in order to observe the effect of E_2 on H_2O_2-induced oxidative stress, the concentration of fetal calf serum in the medium was changed from 10 to 0.5% in the experiments that followed. As shown in
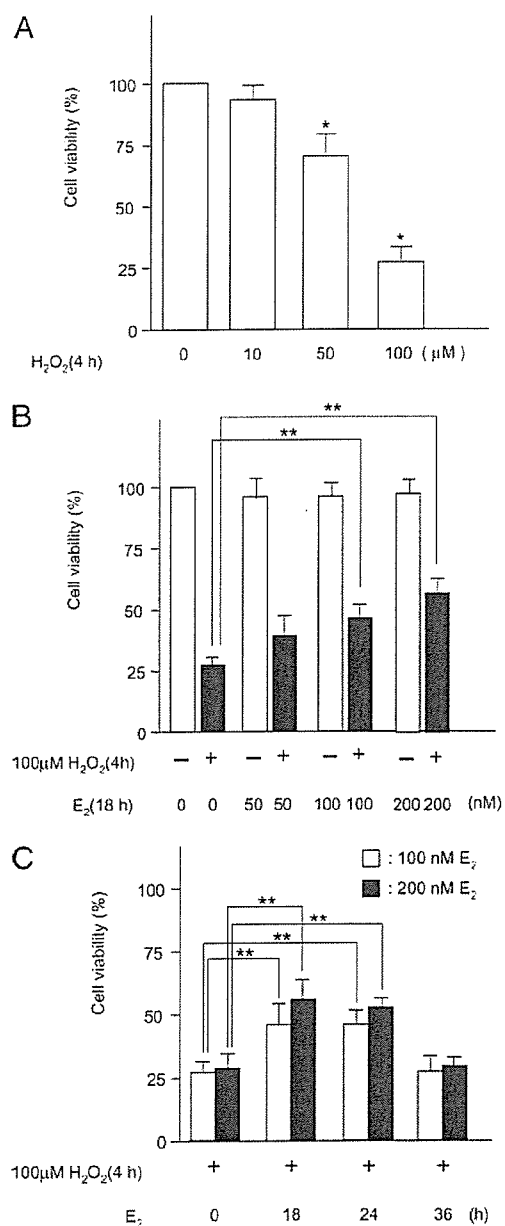
A

B

C

FIGURE 2. **Cytoprotective effect of E_2 on H_2O_2-induced apoptosis.** *A,* viability of H9c2 cells exposed to H_2O_2. Cells were treated with H_2O_2 (0–100 mM) for 4 h, and viability was estimated by the MTT assay. *B,* effect of E_2 on H_2O_2-induced apoptosis. Cells were treated with various concentrations (0–200 nM) of E_2 for 18 h and then with 100 mM H_2O_2 for 4 h. *C,* time course of the cytoprotective effect of E_2. Cells were treated with 100 nM E_2 for 0–36 h and then with 100 mM H_2O_2 for 4 h. The bars express viability (percentage) compared with the cells without H_2O_2. The data are mean ± S.D. of three independent analyses. *, $p < 0.05$ compared with untreated cells; **, $p < 0.05$ compared with cells with H_2O_2 without E_2.

FIGURE 3. **H_2O_2-induced nuclear condensation.** Nuclear condensation was estimated from the PI staining. Cells were treated with 100 nM E_2 for 18 h with or without ICI182,780 (1 μM), a specific inhibitor of ERs, or 0.5 μM PPT (ERα agonist) and then with 100 μM H_2O_2 for 4 h. *A–D,* control cells; *B, E_2; C, E_2* and ICI182,780; *D, E_2* and PPT. *E–H,* cells treated with H_2O_2; *F, E_2; G, E_2* and ICI182,780; *H, E_2* and PPT.

tective effect of E_2 (Fig. 3, *C versus G*). PPT (0.5 mM), a specific inhibitor of ERα, had no apparent influence on the protective effect of E_2 (Fig. 3, *D versus H*). These results suggest that the protective effect against oxidative stress observed on treatment of the cells with E_2 for 18 h involves transcriptional regulation mediated by ERβ through a genomic pathway in this cell line. Unless otherwise indicated, subsequent experiments on the effect of E_2 were done by incubating the cells with 100 nM E_2 for 18 h.

E_2 *Stimulated the Activity of Akt in Response to H_2O_2*—The Akt cascade is known to mediate the survival function. The Akt signal is involved in both the genomic (34) and the nongenomic pathway of E_2 (35). We tested the involvement of Akt in the cytoprotective effect of E_2 in ERβ-positive H9c2 cells. Phosphorylation of Akt (Ser[473]) was promoted by H_2O_2 in 10 min by 1.7-fold, and the control level was reached in 60 min (Fig. 4, *A* and *B*). Prior treatment with E_2 for 18 h resulted in a further increase in the H_2O_2-induced phosphorylation of Akt in 10 min by 4.1-fold, and the phosphorylation continued until 30 min (Fig. 4, *A* and *B, lanes 6 versus lanes 2* and *lanes 7 versus lanes 3*, respectively). ICI182,780 abolished the effect of E_2 (Fig. 4, *C* and *D, lanes 6 versus lanes 4*). The H_2O_2-induced enhancement of Akt activity estimated using GSK3α/β as a substrate was increased by E_2 (Fig. 4, *E* and *F, lanes 5 versus lanes 2* and *lanes 6 versus lanes 3,* respectively), concomitant with the increase in the phosphorylation of Akt. The activity of PDK1, upstream of Akt, was stimulated by H_2O_2; however, E_2 had no apparent effect on the activity of PDK1 (Fig. 4G). The phosphorylation of Akt is regulated by PP2A (18). The activity of PP2A assayed spectrophotometrically using RKpTIRR and *p*-nitrophenylphosphate as substrates was not affected by H_2O_2 and E_2 (Fig. 4H). The data suggest that the change in the activity of PP2A

Fig. 2*A,* the cell viability decreased by H_2O_2, as assessed photometrically with the MTT assay. The cell viability upon treatment with 100 μM H_2O_2 for 4 h was ~27% of the control. Prior treatment of the cells with 100 and 200 nM E_2 for 18 h prevented the H_2O_2 (100 μM)-induced cell damage by 1.4-fold and 1.8-fold of the control level, respectively (Fig. 2*B*). The increase in cell viability caused by E_2 observed in 18 h continued until 24 h and then declined until 36 h (Fig. 2*C*). Morphologically, H_2O_2-induced DNA condensation was observed (Fig. 3, *A versus E*). E_2 protected against DNA condensation (Fig. 3, *B versus F*). ICI182,780, an ER antagonist, abolished the pro-
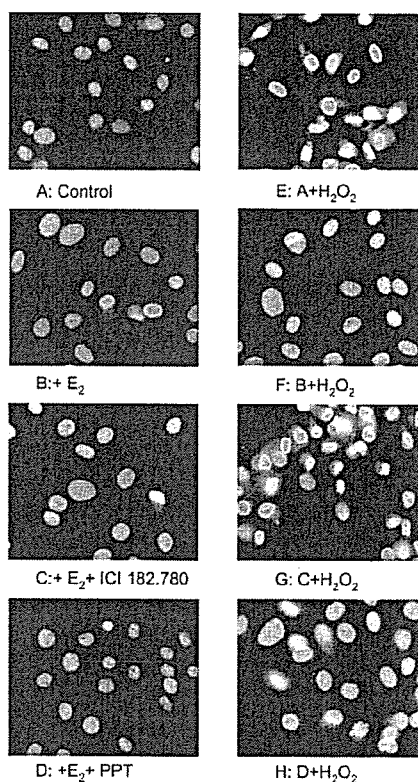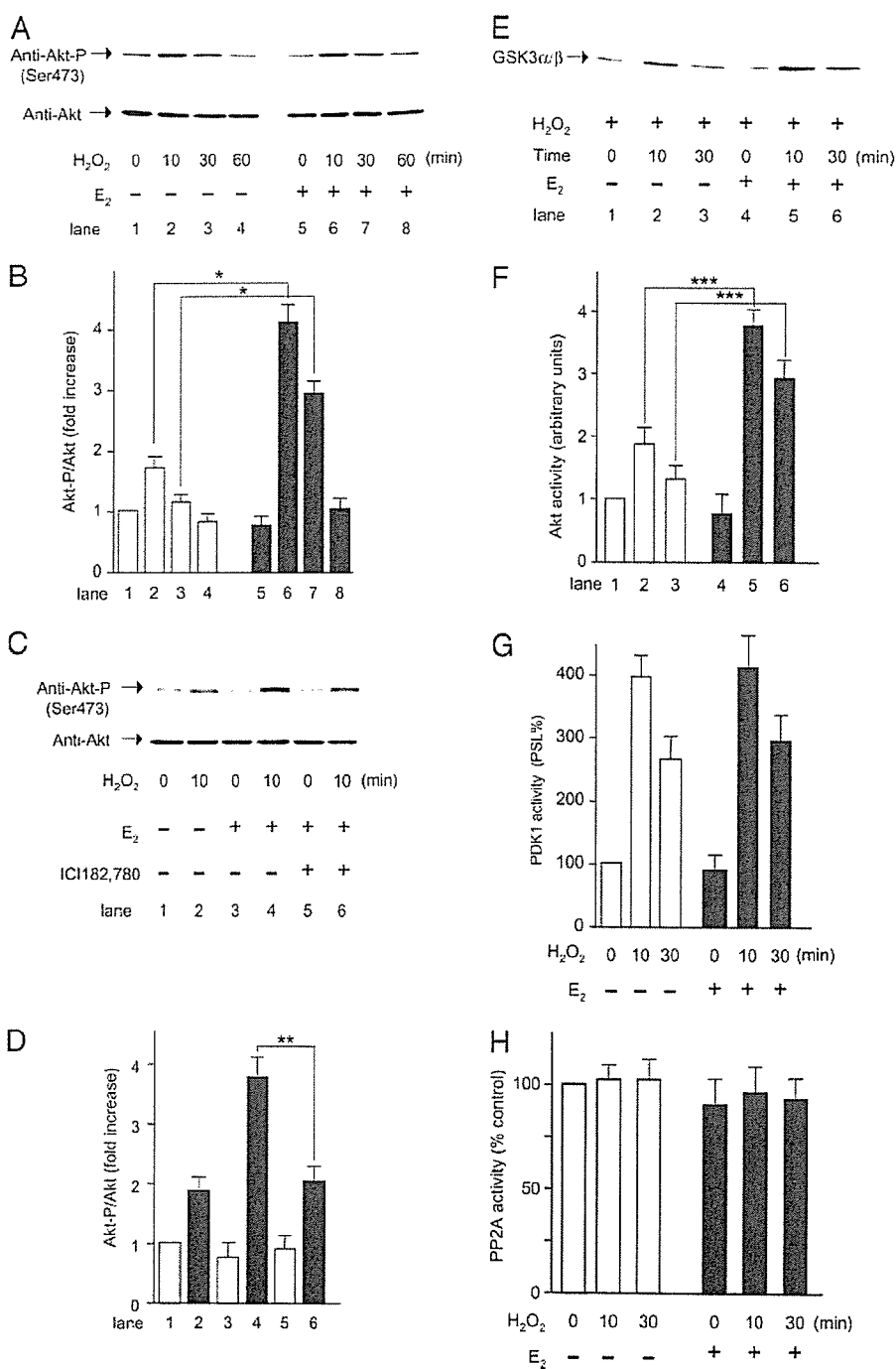
FIGURE 4. **Involvement of phosphorylation of Akt in the cytoprotective effect of E$_2$ against H$_2$O$_2$-induced apoptosis.** *A*, time course of Akt phosphorylation in H9c2 cells under oxidative stress. *C*, cells were treated with 100 nM E$_2$ in the presence or absence of 1 μM ICI182,780 for 18 h and then with 100 μM H$_2$O$_2$ for the period indicated. Phosphorylation of Akt was detected by immunoblot analysis using specific antibodies as described under "Materials and Methods." *B* and *D*, band intensity was estimated densitometrically, and the phosphorylation rates are expressed as the intensity of phosphorylated Akt relative to total Akt (*Akt-p/Akt*). *E*, activity of GSK3α/β. The kinase activity of Akt was measured based on the phosphorylation of GSK3α/β as described under "Materials and Methods." *F*, band intensity was estimated densitometrically, and the phosphorylation rates are expressed as arbitrary units. *G*, the activity of PDK1. The experimental conditions are the same as in *E*. *H*, the activity of PP2A. The activity of PP2A was measured as described under "Materials and Methods." The data are the mean ± S.D. of three independent analyses (*B*, *D*, and *F*). *, $p < 0.05$ compared with cells without E$_2$ at each time point; **, $p < 0.05$ compared with cells with H$_2$O$_2$ and E$_2$ without ICI182,780; ***, $p < 0.05$ compared with cells with H$_2$O$_2$ without E$_2$ at each time point.

is not involved in the up-regulation of the phosphorylation of Akt by E$_2$.

It has been reported that inactive Akt develops a redox-sensitive intramolecular disulfide bond close to its activation loop (18), and recently we found that the redox state of Akt is modulated by H$_2$O$_2$ (19). Fig. 5*A* shows the redox state of Akt assessed by modifying free thiol with AMS. In control cells, Akt existed mostly in an oxidized form (*lane 1*). Treatment of cells with H$_2$O$_2$ resulted in a further increase in an oxidized form of Akt (*lanes 2* and *3*). In the cells treated with E$_2$ for 18 h, Akt existed more in a reduced form (*lane 4*). The reduced form of Akt, once decreased by H$_2$O$_2$ for 30 min, was restored again in 60 min (*lanes 5* and *6*). The data suggested that E$_2$

maintains Akt in a reduced form under oxidative stress. The redox state of Akt is regulated by the GSH/GRX system, and this system protects cells against H$_2$O$_2$-induced apoptosis by preventing the association of Akt with PP2A (19). Then we estimated the effect of E$_2$ on the phosphorylation of Akt in the presence of buthionine sulfoximine (BSO), a specific inhibitor of γ-GCS, or cadmium, an inhibitor of GRX. γ-GCS is a rate-limiting enzyme of GSH synthesis. The effect of E$_2$ on the phosphorylation was abolished both by BSO (Fig. 5*B*) and by cadmium (Fig. 5*C*). These results suggest that E$_2$ increases the levels of GSH/GRX to protect cells against oxidative stress.

E$_2$ Induces the Expression of γ-GCS and GRX—We tested if E$_2$ increases the levels of GSH and GRX. E$_2$ increased the levels of GSH

A

Red
Ox

H$_2$O$_2$	0	30	60	0	30	60
E$_2$	—	—	—	+	+	+
lane	1	2	3	4	5	6

B

Anti- Akt-P → (Ser 473)

Anti-Akt →

lane 1 2 3 4 5 6 7 8

C

Relative intensity (arbitrary units)

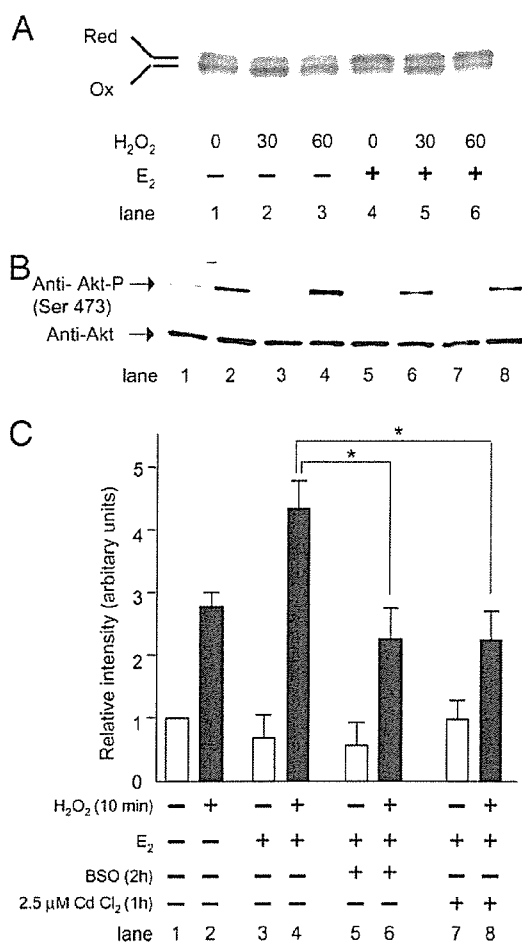| H$_2$O$_2$ (10 min) | — | + | — | + | — | + | — | + |
E$_2$	—	—	+	+	+	+	+	+
BSO (2h)	—	—	—	—	+	+	—	—
2.5 μM Cd Cl$_2$ (1h)	—	—	—	—	—	—	+	+
lane	1	2	3	4	5	6	7	8

FIGURE 5. **E$_2$ retains the redox state of Akt.** *A*, the redox state of Akt was assessed based on mobility shifts of these proteins in an immunoblot analysis as described under "Materials and Methods." The positions of reduced (*Red*) and oxidized (*Ox*) proteins are indicated. The data are from a typical analysis. *B*, effect of modification of the redox on the phosphorylation of Akt was estimated, using 200 μM BSO, a specific inhibitor of γ-GCS (*lanes 5* and *6*), and 2.5 μM cadmium, an inhibitor of GRX (*lanes 7* and *8*). *C*, the activity of Akt phosphorylation is shown as relative intensity in the absence (*open bar*) and presence of H$_2$O$_2$ (*closed bar*). The data are the mean ± S.D. of three independent analyses. *, $p < 0.05$ compared with cells with H$_2$O$_2$ and E$_2$ without inhibitors.

A

☐ E$_2$ ■ E$_2$ + ICI182,780

GSH (nmol /mg protein)

0 12 24   0 12 24
Time (h)

B

γ-GCS heavy subunit →

GAPDH →

E$_2$	—	+	+
ICI182,780	—	—	+
lane	1	2	3

C

γ-GCS / GAPDH (% control)

lane 1 2 3

D

β-Actin →

GRX →

E$_2$	—	+	+
ICI182,780	—	—	+
lane	1	2	3

E

GRX/β-Actin (% control)

lane 1 2 3

FIGURE 6. **GSH synthesis and GRX.** Effects of E$_2$ on levels of GSH, the γ-GCS heavy subunit, and GRX were estimated in the presence or absence of ICI182,780, as described under "Materials and Methods." *A*, cells were treated with 100 nM E$_2$ for 0–24 h, and the levels of GSH in the cell lysates were estimated. Cells were incubated with 100 nM E$_2$ for 6 h for the analysis of the expression of the γ-GCS heavy subunit by Northern blotting (*B*) and that of GRX by RT-PCR (*D*). The expression of γ-GCS was expressed as relative intensity (percentage of control) (*C*), and that of GRX was expressed as the intensity of GRX/β-actin (*E*). Each datum is a mean ± S.D. of three independent analyses. *, $p < 0.05$ compared with untreated cells.

(Fig. 6*A*). The level of GSH was 24.8 ± 4.0 nmol/10^6 cells in control cells and 38.5 ± 5.2 nmol/10^6 cells in cells treated with 100 nM E$_2$ for 18 h. The level of GSSG in the control cells was ~2 nmol/10^6 cells and was not changed by E$_2$ treatment (data not shown). The expression of γ-GCS was up-regulated by 100 nM E$_2$ by 1.6-fold in 18 h (Fig. 6, *B* and *C*). Similarly, 100 nM E$_2$ increased the expression of GRX by 1.8-fold in 18 h (Fig. 6, *D* and *E*). ICI182,780 abolished the E$_2$-dependent up-regulation of GSH synthesis as well as GRX synthesis (Fig. 6, *A–E*). It is suggested that the redox state of Akt is regulated by an E$_2$-dependent enhancement of the GRX/GSH system.

The Gene Promoter Activity of GRX Is Regulated by E$_2$ via an EpRE-like Element—As reported by Montano *et al.* (7), the expression of the γ-GCS heavy (catalytic) subunit is up-regulated by E$_2$ via an EpRE (5'-(G/A)TGACNNNGC(G/A)-3'), not by an ERE. To investigate the mechanism of the transcriptional regulation of GRX by E$_2$, we used a 2.0-kb genomic fragment containing the promoter region of GRX inserted into a luciferase vector, pGL3 Basic. The promoter region contains no apparent ERE or EpRE. There were two EpRE-like sites (EpRE-like 1 (−1380 to −1370; GTGACTCAGAA) and EpRE-like 2 (−347 to −337; GTGAGTAAGCA)) and Sp1 (−1217 to −1208, GCCCCGC-
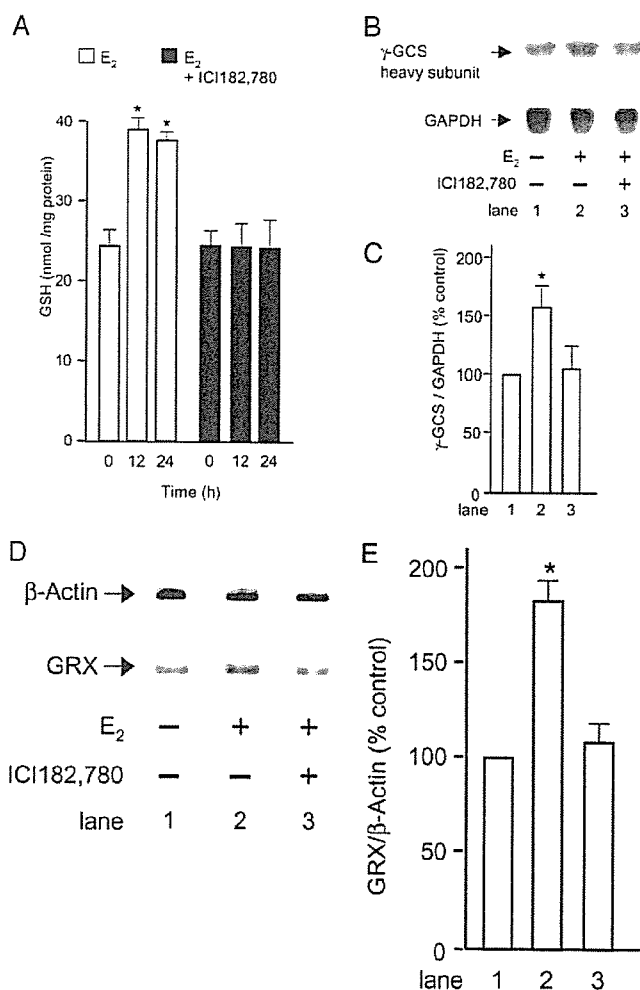
CTC). The luciferase activity of the cells previously treated with E$_2$ for 18 h was almost lost when the EpRE-like 1 site was deleted or mutated (Fig. 7). Deletion of EpRE-like 2 or Sp1 had no apparent effect on the E$_2$-induced up-regulation of the luciferase activity.

E$_2$ Up-regulated the ERβ-EpRE-like 1 Complex Formation—To investigate the importance of the EpRE-like elements in the E$_2$-induced expression of GRX, an electrophoretic mobility shift assay was performed with nuclear extracts from the cells treated with E$_2$ for 18 h using ^{32}P-labeled oligonucleotides designed for EpRE-like 1. As shown in Fig. 8, a protein-DNA complex of EpRE-like 1 (*lane 2*) increased by E$_2$ (*lane 3*) and appeared in the presence of an excess of unlabeled probe (*lane 4*), or ^{32}P-labeled probe with the disabled mutant for EpRE-like 1 (*lane 5*). The addition of the anti-ERβ antibody caused the ERβ-DNA-binding complex to disappear (*lane 12*), indicating the involvement of ERβ as a transcription factor that bound to the EpRE-like 1 site. The EpRE-like 1 of GRX did not bind with Nrf2, Sp1, c-Jun, or c-Fos (*lanes 9–11*), different from the EpRE site of the γ-GCS heavy subunit (7). On the other hand, neither EpRE-like 2 site nor the Sp1 site was stimulated by E$_2$ (data not shown).

FIGURE 7. **The EpRE-like element is important for the E_2-dependent induction of the GRX promoter in H9c2 cells.** *Left,* schematic representation of luciferase vector constructs for the human GRX promoter. Each luciferase vector construct was generated as described under "Materials and Methods." *Right,* luciferase activity of the vector constructs for the human GRX gene promoter in H9c2 cells. The cells were transiently transfected with the GRX promoter-luciferase gene fusion plasmids. After the transfection, luciferase activity was assayed with cellular extracts as described under "Materials and Methods." Each value represents the mean of at least three independent experiments, and the S.D. was always within 10% of the mean. *, $p < 0.05$ compared with control.
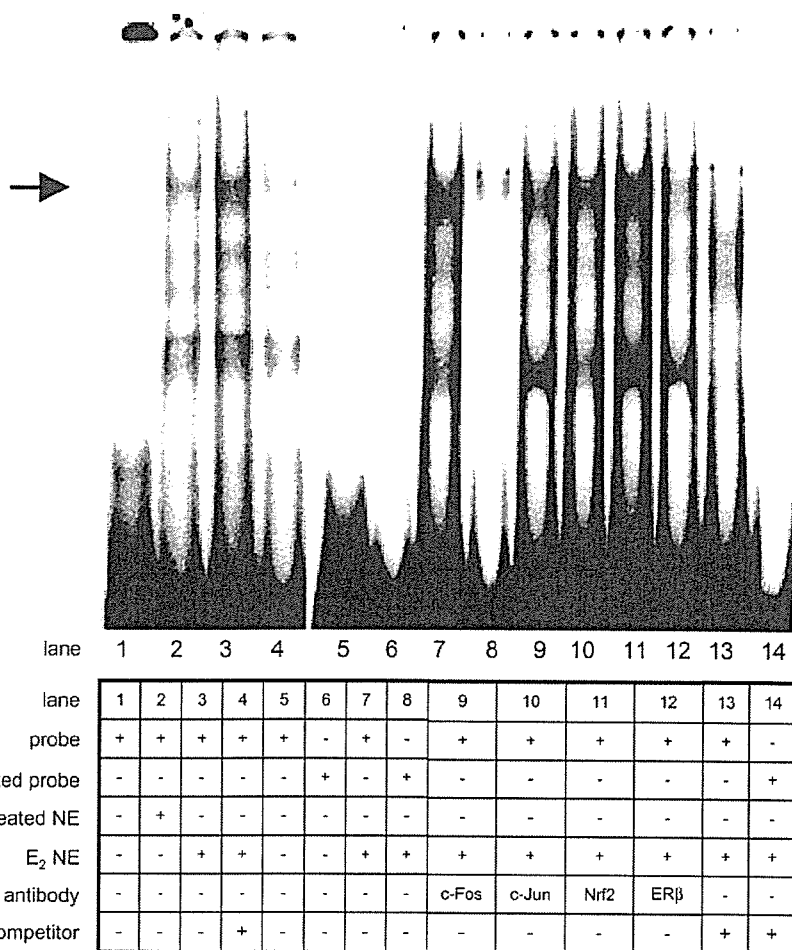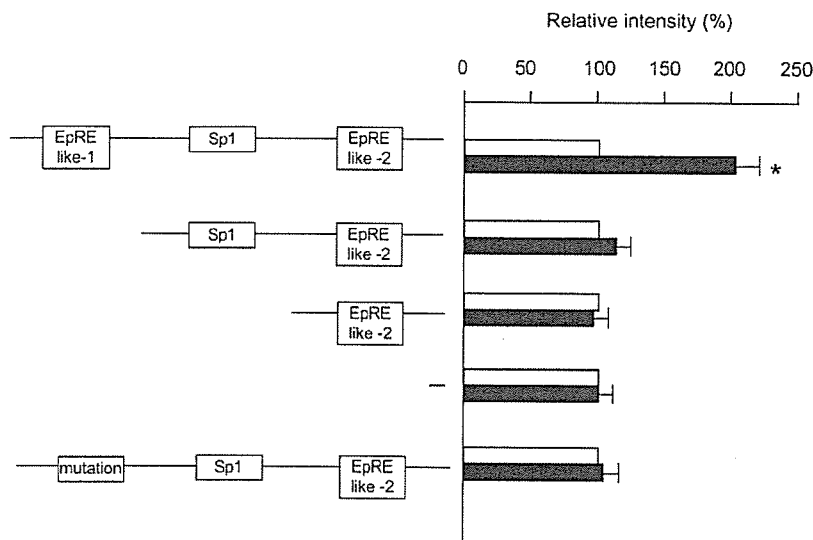

FIGURE 8. **The EpRE-like 1 element is responsive to E_2 in electrophoretic mobility shift assays.** H9c2 cells were incubated with 100 nM E_2 for 18 h, and the nuclear extracts were prepared as described under "Materials and Methods." ^{32}P-Labeled oligonucleotides specific to EpRE-like elements 1 and 2 of the GRX gene promoter were prepared and incubated with each nuclear extract and then subjected to a 5% nondenatured PAGE. In *lanes 1, 5,* and *6,* the nuclear extract (*NE*) was free. In *lanes 6, 8,* and *14,* ^{32}P-labeled mutant oligonucleotides were used. In *lanes 9–12,* +*Ab,* specific antibodies were added to the reaction mixture during the binding reaction for the supershift assay. *Arrowhead,* protein-DNA complex.

lane	1	2	3	4	5	6	7	8	9	10	11	12	13	14
probe	+	+	+	+	+	-	+	-	+	+	+	+	+	-
mutated probe	-	-	-	-	-	+	-	+	-	-	-	-	-	+
untreated NE	-	+	-	-	-	-	-	-	-	-	-	-	-	-
E_2 NE	-	-	+	+	-	-	+	+	+	+	+	+	+	+
antibody	-	-	-	-	-	-	-	-	c-Fos	c-Jun	Nrf2	ERβ	-	-
competitor	-	-	-	+	-	-	-	-	-	-	-	-	+	+

Important Role of ERβ in Other Cells—To further confirm the role of ERβ in protection against oxidative stress through redox regulation of Akt, we employed human breast cancer cells, SK-BR-3 and MDA-MB-231 cells. As shown in Fig. 9A, an RT-PCR analysis revealed that these cells mainly expressed ERβ mRNA. A stimulatory effect of E_2 on the activity of Akt was observed in these cells (Fig. 9, *B* and *C*). However, ICI182,780 abolished the protective effect of E_2 (Fig. 9, *B* and *C*). E_2 induced the expression of GRX (Fig. 9, *D* and *E*). The results suggested that the cytoprotective effect of E_2 is mediated through redox regulation of Akt activity in ERβ-expressing cells.

DISCUSSION

ERβ-mediated Cytoprotection against Oxidative Stress—Estrogenic hormones are required for the growth and differentiation of female
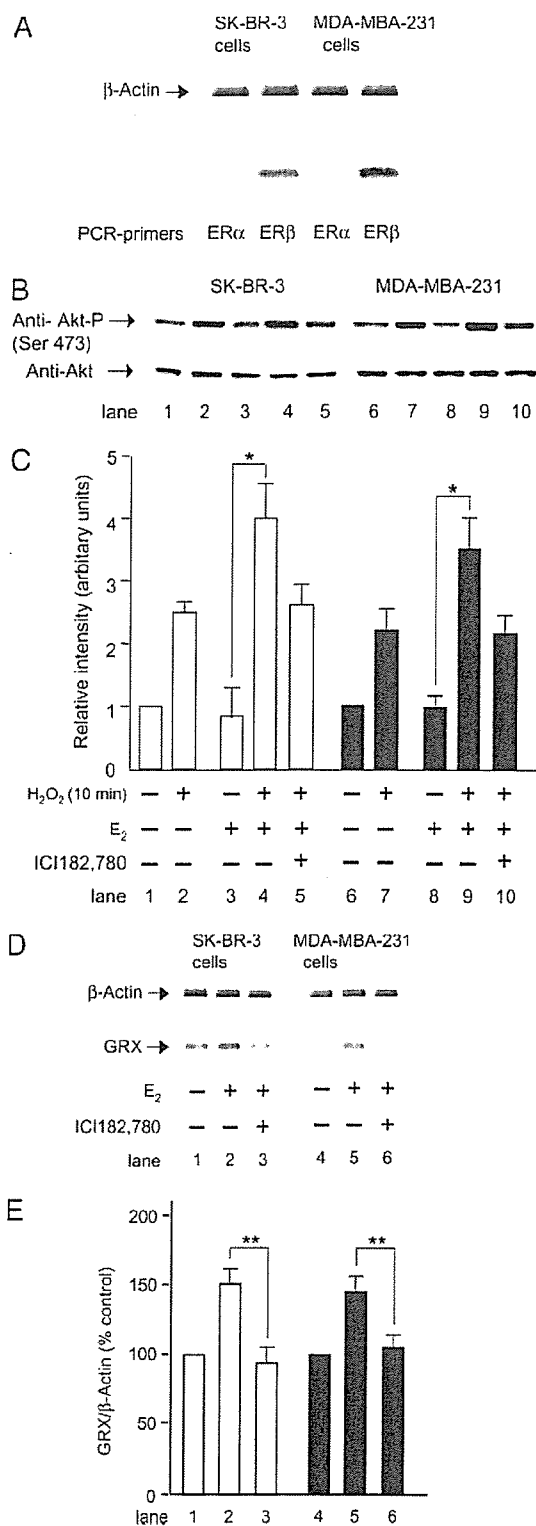
FIGURE 9. **Protective effect of E_2 in other cell lines.** The effect of E_2 was studied using ERβ-expressing human breast cancer SK-BR-3 cells and MDA-MB-231 cells. A, expression of ERs. The gene expression of ERs was estimated by RT-PCR analysis as described in the legend to Fig. 1. B, phosphorylation of Akt. The effect of E_2 on the phosphorylation of Akt under oxidative stress was estimated by immunoblot analysis using specific antibodies as described under "Materials and Methods." C, band intensity was estimated densito-metrically, and the phosphorylation rates are expressed as the relative intensity of phos-phorylated Akt to total Akt (Akt-p/Akt). The data are the mean $\pm$ S.D. of three independ-ent analyses (B and D). D, gene expression of GRX. The effect of E_2 on levels of the GRX was estimated as described under "Materials and Methods." E, band intensity was

reproductive tissues, contribute to male fertility, and play a role in main-taining cardiovascular, skeletal, and neural cell functions (9). Estrogen has been widely used to regulate fertility, relieve postmenopausal symp-toms, and decrease the incidence and recurrence of mammary tumors. The ERs were the first members of the nuclear receptor family to be identified. ERα has been well characterized and plays a major role in E_2-mediated genomic actions in both reproductive and nonreproduc-tive tissues. ERα-mediated cytoprotection against oxidative stress-in-duced cell damage has been reported in neurological cells (33, 34) and breast cancer cells (35). On the other hand, the role of ERβ is not well understood. A report using microarray analyses showed that most of the genes regulated by ERβ are distinct from those regulated by ERα in response to E_2 and selective estrogen receptor modulators (36). ERβ regulates plasminogen activator inhibitor-1 in endothelial cells, and a clinical evaluation of ERβ was suggested as a prognostic or predictive factor of drug resistance in breast cancer (37). These results suggest a significant role for ERβ in the regulation of cellular function, although the function of ERβ and its precise mechanism are still unclear (3). Thus, this is the first report aimed at the significant role of ERβ-medi-ated signals of E_2 in redox regulation in response to oxidative stress.

Involvement of Akt in the Cytoprotection of E2 Mediated by ERβ— The importance of Akt has been suggested in the cytoprotective effect of E_2 against oxidative stress. This effect of E_2 was rapid and nongenomic in neurological cells (38), vascular endothelial cells (39), and ovarian cancer cells (40). On the other hand, Stoica et al. (41) reported that ERα-mediated signals up-regulated the expression of Akt in ERα-posi-tive MCF-7 breast cancer cells. They also demonstrated that Akt-medi-ated signals up-regulated the expression of ERα in these cells, suggesting that Akt plays a central role in the growth and survival of breast cancer cells; however, the mechanism by which Akt is activated by E_2 was not fully characterized.

In the present study, we were interested in the possible involvement of Akt signals in the ERβ-mediated anti-apoptotic effect against oxida-tive stress. We employed H9c2 cells that apparently express only ERβ (Fig. 1). We found that 1) H_2O_2-induced apoptosis was prevented when the cells were incubated with E_2 for over 18 h; 2) the anti-oxidative effect of E_2 was mediated by a genomic pathway through ERβ; and 3) E_2 retained the level of phosphorylated Akt in response to H_2O_2 via the GSH/GRX system.

Role of the GSH/GRX System in ERβ-mediated Akt Signals—We reported previously a role for the GRX/GSH system in the regulation of Akt phosphorylation (19). Akt is a Ser/Thr protein kinase with anti-apoptotic and oncogenic activities. Akt is activated through a growth factor receptor-mediated activation of the phosphatidylinositol 3-ki-nase pathway (21). The unphosphorylated form of Akt is virtually inac-tive, and phosphorylation at Thr[308] and Ser[473] stimulates its activity. Inactivation of Akt also occurs via dephosphorylation of the two phos-phorylation sites by PP2A (23, 24). The activation of Akt contributes to the survival of H_2O_2-treated cells (25). H_2O_2 induces oxidation of Akt at Cys[297] and Cys[311], and the oxidized form of Akt can be dephosphoryl-ated by PP2A (19). PP2A is a major Ser/Thr phosphatase implicated in the regulation of many cellular processes, including the regulation of different signal transduction pathways, cell cycle progression, DNA rep-lication, gene transcription, and protein translation (42). Yasukawa et al. have reported that Akt is also inactivated by S-nitrosylation at Cys[224] in NO donor-treated cells (43). Furthermore, we recently reported that the phosphorylation of Akt is down-regulated by cytoplasmic calcium (32).

Calcium induced the expression of the PP2A catalytic subunit mediated by cAMP via the cAMP-response element. In the present study, the activity and the expression of the anti-PP2A catalytic C subunit did not change upon treatment with E_2 in H9c2 cells (Fig. 4H), suggesting that the modulation of calcium levels may not be involved. Inactivation by ROS of protein phosphatases, such as protein-tyrosine phosphatase 1B (44), mitogen-activated protein kinase (MAPK) phosphatases (45), and PP2A (46), has been reported. In the present study, the activity of PP2A was not changed by H_2O_2 (Fig. 4H), suggesting that inactivation of PP2A by ROS is not involved. The redox state of Akt is regulated by GSH/GRX (19). Oxidation of Akt at Cys[297] and Cys[311] facilitates the association of PP2A, leading to the dephosphorylation of Akt. However, the activity of Akt is not affected by the oxidation. In the present study, oxidation of Akt was observed in the medium with 0.5% fetal calf serum in the absence of H_2O_2, and after the treatment with H_2O_2, the oxidation of Akt continued for 60 min. In such conditions, E_2 maintained Akt in the reduced form (Fig. 5). This suggested that E_2 potentiates the functions of the GSH/GRX system. The GSH/GRX system regulates many signals, such as ASK-1, NF1, PTP1B, protein kinase C, and protein kinase A (49). The present study indicates for the first time that ERβ-mediated signaling via E2 up-regulates the activity of the GSH/GRX system to stimulate Akt and protects cells against oxidative stress.

Up-Regulation of γ-GCS and GRX by E_2—The ERα-mediated expression of antioxidants in response to oxidative stress has been reported. Genomic effects on the expression of antioxidant enzymes reported were Mn-SOD (4, 6), Cu,Zn-SOD (6), COX-1 (47), and COX-2 (5). Induction of GRX expression by E_2 was reported in bovine aortic endothelial cells (48) and in female mice (34). These reports suggested a potential contribution of TRX and GRX to the protection of cells against oxidative stress. As to ERβ, the expression of γ-GCS induced by E_2 was reported to be mediated by ERβ (7) in breast epithelial cell lines.

In the present study, we found that the expression of both GRX and γ-GCS is up-regulated by E_2 in ERβ-expressing cells. Data on the induction of the γ-GCS heavy subunit (Fig. 6, B and C) together with an increase in the level of GSH obtained here (Fig. 6A) is consistent with such a contribution. Furthermore, E_2 up-regulated the expression of GRX (Fig. 6, D and E). Elevated levels of both GSH and GRX were necessary to retain the reduced form of Akt. BSO abolished the effect of E_2 on the phosphorylation of Akt (Fig. 5B), and cadmium also abolished the effect of E_2 (Fig. 5C). The up-regulation of γ-GCS as well as GRX expression by E_2 was abolished by ICI182,780 (Fig. 6, A–E), suggesting involvement of the ERβ-mediated genomic effect of E_2. The possible role of ERβ in the cytoprotection against oxidative stress was supported by the results obtained using other ERβ-expressing cells (Fig. 9). Although involvement of ERα in the cytoprotective effect of E_2 cannot be ruled out in these cells, it is suggested that the GRX/GSH system is involved in the cytoprotective and genomic effects of E_2 on the redox state of Akt, a pathway that is mediated, at least in part, by ERβ. This mechanism may also play an antiapoptotic role in cancer cells during carcinogenesis or chemotherapy. A difference in the distribution of ERα and ERβ was reported (3, 27, 50, 51). ERα and ERβ differ in the distribution in tissue cells and how they regulate cell proliferation and apoptosis, which may provide some insight into the tissue-specific functions and interplay between the two receptors.

The role of the GSH/GRX redox system in the antiapoptotic effect of E_2 was studied further. In the present study, we found that the induction of GRX expression by E_2 is mediated by an EpRE-like 1 element (Figs. 7 and 8). The human GRX promoter employed here possessed no apparent ERE or EpRE but had two EpRE-like sites. Interestingly, one of these

sites, EpRE-like 1, bound to ERβ and promoted the transcriptional activity of GRX. Transcription of the GRX gene was increased by E_2 but decreased by anti-ERβ antibody. However, EpRE-like 1 did not bind to Nrf-2 or AP-1. This element may be a novel kind of ERE. In summary, E_2 has a cytoprotective effect against oxidative stress in H9c2 cells expressing ERβ. The genomic effect of E_2 on the GSH/GRX redox system potentiates Akt activity, a mechanism that may also play an antiapoptotic role in cancer cells during carcinogenesis or chemotherapy.

REFERENCES
1. Berlett, S. B., and Stadtman, E. R. (1997) *J. Biol. Chem.* **272**, 20313–20316
2. Finkel, T., and Holbrook, N. J. (2000) *Nature* **408**, 239–247
3. Yang, S. H., Liu, R., Perez, E. J., Wen, Y., Stevens, S. M., Jr., Valencia, T., Brun-Zinkernagel, A. M., Prokai, L., Will, Y., Dykens, J., Koulen, P., and Simpkins, J. W. (2004) *Proc. Natl. Acad. Sci. U. S. A.* **101**, 4130–4135
4. Baba, T., Shimizu, T., Suzuki, Y., Ogawara, M., Isono, K., Koseki, H., Kurosawa, H., and Shirakawa, T. (2005) *J. Biol. Chem.* **280**, 16417–16426
5. Egan, K. M., Lawson, J. A., Fries, S., Koller, B., Rader, D. J., Smyth, E. M., and Fitzgerald, G. A. (2004) *Science* **306**, 1954–1957
6. Strehlow, K., Rotter, S., Wassmann, S., Adam, O., Grohe, C., Laufs, K., Bohm, M., and Nickenig, G. (2003) *Circ. Res.* **93**, 170–177
7. Montano, M. M., Deng, H., Liu, M., Sun, X., and Singal, R. (2004) *Oncogene* **23**, 2442–2453
8. Beato, M., Herrlich, P., and Schutz, G. (1995) *Cell* **83**, 851–857
9. Schultz, J. R., Petz, L. N., and Nardulli, A. M. (2005) *J. Biol. Chem.* **280**, 347–354
10. Foster, C., Keitz, S., Hultenby, K., Warner, M., and Gustafsson, J. A. (2004) *Proc. Natl. Acad. Sci. U. S. A.* **101**, 14234–14239
11. Holmgren, A. (1989) *J. Biol. Chem.* **264**, 13963–13966
12. Meister, A. (1973) *Science* **180**, 33–39
13. Holmgren, A. (1976) *Proc. Natl. Acad. Sci. U. S. A.* **73**, 2275–2279
14. Gan, Z.-R., and Wells, W. W. (1986) *J. Biol. Chem.* **261**, 996–1001
15. Gravina, S. A., and Mieyal, J. J. (1993) *Biochemistry* **32**, 3368–3376
16. Song, J. J., Rhee, J. G., Suntharalingam, M., Walsh, S. A., Spitz, D. R., and Lee, Y. J. (2002) *J. Biol. Chem.* **277**, 46566–46575
17. Song, J. J., and Lee, Y. J. (2003) *Biochem. J.* **373**, 845–853
18. Murata, H., Ihara, Y., Nakamura, H., Yodoi, J., Sumikawa, K., and Kondo, T. (2003) *J. Biol. Chem.* **278**, 50226–50233
19. Huang, X., Begley, M., Morgenstern, K. A., Gu, Y., Rose, P., Zhao, H., and Zhu, X. (2003) *Structure (Camb.)* **11**, 21–30
20. Brazil, D. P., and Hemmings, B. A. (2001) *Trends Biochem. Sci.* **26**, 657–664
21. Franke, T. F., Hornik, C. P., Segev, L., Shostak, G. A., and Sugimoto, C. (2003) *Oncogene* **22**, 8983–8998
22. Luikenhuis, S., Perrone, G., Dawes, I. W., and Grant, C. M. (1998) *Mol. Biol. Cell* **9**, 1081–1091
23. Andjelkovic, M., Jakubowicz, T., Cron, P., Ming, X. F., Han, J. W., and Hemmings, B. A. (1996) *Proc. Natl. Acad. Sci. U. S. A.* **93**, 5699–5704
24. Pham, F. H., Sugden, P. H., and Clerk, A. (2000) *Circ. Res.* **86**, 1252–1258
25. Hayashi, S., Hajiro-Nakanishi, K., Makino, Y., Eguchi, H., Yodoi, J., and Tanaka, H. (1997) *Nucleic Acids Res.* **25**, 4035–4040
26. Goto, S., Kamada, K., Soh, Y., Ihara, Y., and Kondo, T. (2002) *Jpn. J. Cancer Res.* **93**, 1047–1056
27. Tamaru, N., Hishikawa, Y., Ejima, K., Nagasue, N., Inoue, S., Muramatsu, M., Hayashi, T., and Koji, T. (2004) *Lab. Invest.* **84**, 1460–1471
28. Kobayashi, T., Kishigami, S., Sone, M., Inokuchi, H., Mogi, T., and Ito, K. (1997) *Proc. Natl. Acad. Sci. U. S. A.* **94**, 11857–11862
29. Iida, T., Kijima, H., Urata, Y., Goto, S., Ihara, Y., Oka, M., Kohno, S., Scanlon, K. J., and Kondo, T. (2001) *Cancer Gene Ther.* **8**, 803–814
30. Sambrook, J., Fritsch, E. F., and Maniatis, T. (1989) *Molecular Cloning: A Laboratory Manual*, 2nd Ed., Cold Spring Harbor Laboratory, Cold Spring Harbor, NY
31. Padilla, C. A., Bajalica, S., Lagercrantz, J., and Holmgren, A. (1996) *Genomics* **32**, 455–457
32. Yasuoka, C., Ihara, Y., Ikeda, S., Miyahara, Y., Kondo, T., and Kohno, S. (2004) *J. Biol. Chem.* **279**, 51182–51192
33. Prokai, L., Prokai-Tatrai, K., Perjesi, P., Zharikova, A. D., Perez, E. J., Liu, R., and Simpkins, J. W. (2003) *Proc. Natl. Acad. Sci. U. S. A.* **100**, 11741–11746
34. Kenchappa, R. S., Diwakar, L., Annepu, J., and Ravindranath, V. (2004) *FASEB J.* **18**, 1102–1104
35. Fernando, R. I., and Wimalasena, J. (2004) *Mol. Biol. Cell* **15**, 3266–3284

36. Tee, M. K., Rogatsky, I., Tzagarakis-Foster, C., Cvoro, A., An, J., Christy, R. J., Yamamoto, K. R., and Leitman, D. C. (2004) *Mol. Biol. Cell* 15, 1562–1572

37. Smith, L. H., Coats, S. R., Coats, S. R., Qin, H., Petrie, M. S., Covington, J. W., Su, M., Eren, M., and Vaughan, D. E. (2004) *Circ. Res.* 95, 269–275

38. Yu, X., Rajala, R. V., McGinnis, J. F., Li, F., Anderson, R. E., Yan, X., Li, S., Elias, R. V., Knapp, R. R., Zhou, X., and Cao, W. (2004) *J. Biol. Chem.* 279, 13086–13094

39. Lu, Q., Pallas, D. C., Surks, H. K., Baur, W. E., Mendelsohn, M. E., and Karas, R. H. (2004) *Proc. Natl. Acad. Sci. U. S. A.* 101, 17126–17131

40. Mabuchi, S., Ohmichi, M., Kimura, A., Nishio, Y., Arimoto-Ishida, E., Yada-Hashimoto, N., Tasaka, K., and Murata, Y. (2004) *Endocrinology* 145, 49–58

41. Stoica, G. E., Franke, T. F., Moroni, M., Mueller, S., Morgan, E., Iann, M. C., Winder, A. D., Reiter, R., Wellstein, A., Martin, M. B., and Stoica, A. (2003) *Oncogene* 22, 7998–8011

42. Janssens, V., Goris, J., and Van Hoof, C. (2005) *Curr. Opin. Genet. Dev.* 15, 34–41

43. Yasukawa, T., Tokunaga, E., Ota, H., Sugita, H., Martyn, J. A., and Kaneki, M. (2005) *J. Biol. Chem.* 280, 7511–7518

44. Salmeen, A., Andersen, J. N., Myers, M. P., Meng, T. C., Hinks, J. A., Tonks, N. K., and Barford, D. (2003) *Nature* 423, 769–773

45. Kamata, H., Honda, S., Maeda, S., Chang, L., Hirata, H., and Karin, M. (2005) *Cell* 120, 649–661

46. Rao, R. K., and Clayton, L. W. (2002) *Biochem. Biophys. Res. Commun.* 293, 610–616

47. Gibson, L. L., Hahner, L., Osborne-Lawrence, S., German, Z., Wu, K. K., Chambliss, K. L., and Shaul, P. W. (2005) *Circ. Res.* 96, 518–525

48. Ejima, K., Nanri, H., Araki, M., Uchida, K., Kashimura, M., and Ikeda, M. (1999) *Eur. J. Endocrinol.* 140, 608–613

49. Shelton, M. D., Chock, P. B., and Mieyal, J. J. (2005) *Antioxid. Redox Signal.* 7, 348–366

50. Helguero, L. A., Fauld, M. H., Guslafsson, J. A., and Haldosen, L. A. (2005) *Oncogene* 24, 6605–6616

51. Connor, E. E., Wood, D. L., Sonstegard, T. S., da Mota, A. F., Bennet, G. L., and Williams, J. L. (2005) *J. Endocrinol.* 185, 593–603

The Journal of Biological Chemistry

Glutaredoxin Modulates Platelet-derived Growth Factor-dependent Cell Signaling by Regulating the Redox Status of Low Molecular Weight Protein-tyrosine Phosphatase*[S]

Munetake Kanda[‡§1], Yoshito Ihara[‡1,2], Hiroaki Murata[‡], Yoshishige Urata[‡], Takaaki Kono[‡], Junji Yodoi[¶], Shinji Seto[§], Katsusuke Yano[§], and Takahito Kondo[‡]

From the ‡Department of Biochemistry and Molecular Biology in Disease, Atomic Bomb Disease Institute and §Department of Third Internal Medicine, Nagasaki University Graduate School of Biomedical Sciences, Nagasaki 852-8523, Japan and ¶Department of Biological Responses, Institute for Viral Research, Kyoto University, Kyoto 606-8507, Japan

Glutaredoxin (GRX) is a glutathione-disulfide oxidoreductase involved in various cellular functions, including the redox-dependent regulation of certain integral proteins. Here we demonstrated that overexpression of GRX suppressed the proliferation of myocardiac H9c2 cells treated with platelet-derived growth factor (PDGF)-BB. After stimulation with PDGF-BB, the phosphorylation of PDGF receptor (PDGFR) β was suppressed in GRX gene-transfected cells, compared with controls. Conversely, the phosphorylation was enhanced by depletion of GRX by RNA interference. In this study we focused on the role of low molecular weight protein-tyrosine phosphatase (LMW-PTP) in the dephosphorylation of PDGFRβ via a redox-dependent mechanism. We found that depletion of LMW-PTP using RNA interference enhanced the PDGF-BB-induced phosphorylation of PDGFRβ, indicating that LMW-PTP works for PDGFRβ. The enhancement of the phosphorylation of PDGFRβ was well correlated with inactivation of LMW-PTP by cellular peroxide generated in the cells stimulated with PDGF-BB. In vitro, with hydrogen peroxide treatment, LMW-PTP showed decreased activity with the concomitant formation of dithiothreitol-reducible oligomers. GRX protected LMW-PTP from hydrogen peroxide-induced oxidation and inactivation in concert with glutathione, NADPH, and glutathione disulfide reductase. This strongly suggests that retention of activity of LMW-PTP by enhanced GRX expression suppresses the proliferation of cells treated with PDGF-BB via enhanced dephosphorylation of PDGFRβ. Thus, GRX plays an important role in PDGF-BB-dependent cell proliferation by regulating the redox state of LMW-PTP.

The redox status of sulfhydryl groups in proteins plays an important role in the regulation of cellular functions such as the synthesis and folding of proteins and regulation of the structure and activity of enzymes, receptors, and transcription factors. To maintain the cellular thiol-disulfide redox status under reducing conditions, living cells possess two major systems, the thioredoxin (TRX)[3]/thioredoxin reductase system and the glutathione (GSH)/glutaredoxin (GRX) system (1).

GRX, also known as thiol transferase, was first discovered as a GSH-dependent hydrogen donor for ribonucleotide reductase in Escherichia coli mutants lacking TRX (2). GRX catalyzes the reduction of protein disulfide via a disulfide exchange reaction by utilizing the active site Cys-Pro-Tyr-Cys with a dithiol mechanism involving both active-site thiols (3). In addition, GRX has a unique ability to reduce protein-S-S-glutathione mixed disulfide (deglutathionylation) or to participate in its formation (glutathionylation) through a monothiol mechanism, which requires only the more N-terminal active site Cys (3, 4). Oxidized GRX is selectively recycled to the reduced form by GSH with the formation of glutathione disulfide (GSSG) and regeneration of GSH through coupling with NADPH and GSSG reductase, a system termed the GSH-regenerating system (5, 6). These characteristic interactions with GSH distinguish GRX from TRX, which favors intramolecular disulfide substrates and is turned over by NADPH and thioredoxin reductase independent of GSH. Functional overlap or cross-talk between the two systems, however, has been indicated (7, 8).

Mammalian GRX is known to have two isoforms, GRX1 and GRX2 (4). GRX1 is a cytosolic form of GRX. GRX1 and S-glutathionylation are thought to be involved in a variety of cellular events such as signal transduction, stress response, and metabolic regulation by regulating the redox status of various cellular proteins including human immunodeficiency virus-1 protease (9), glyceraldehyde-3-phosphate dehydrogenase (10), nuclear factor I (11), ASK1 (12), EphA2 kinase (13), actin (14), Ras (15), tubulin (16), tau and microtubule-associated protein-2 (17), annexin

[3] The abbreviations used are: TRX, thioredoxin; AMS, 4-acetamido-4'-maleimidylstilbene-2,2'-disulfonic acid; DTT, dithiothreitol; GRX, glutaredoxin; GST, glutathione S-transferase; LMW-PTP, low molecular weight-protein-tyrosine phosphatase; PTPI, PTP inhibitor; NAC, N-acetyl-L-cysteine; PDGF, platelet-derived growth factor; PDGFR, PDGF receptor; ROS, reactive oxygen species; FCS, fetal calf serum; siRNA, small interfering RNA; SHP, Src homology 2-containing protein-tyrosine phosphatase; DEP-1, density-enhanced protein-tyrosine phosphatase-1; TC-PTP, T-cell protein-tyrosine phosphatase.

A2 (18), and protein-tyrosine phosphatase 1B (4, 19). We also have reported that GRX plays an important role in protecting cells from apoptosis by regulating the redox status of Akt/protein kinase B (20). The other form of GRX, GRX2, is distributed in the mitochondria and nucleus and also functions as part of a cellular antioxidant defense system by regulating the redox status of mitochondrial proteins such as complex I protein (21–23).

Platelet-derived growth factor (PDGF) is a major mitogen for connective tissue cells and certain other cell types. PDGF is a family of homo- and heterodimers of disulfide-bonded polypeptide chains A, B, C, and D (*i.e.* PDGF-AA, BB, CC, DD, and AB) (24). PDGFs bind to two cell-surface receptor-tyrosine kinases, PDGF receptor (PDGFR) α and β. The PDGF molecules are bivalent, and PDGF-dependent activation of receptors causes a mitogenic signal transduction through the phosphorylation of specific tyrosines in the receptors. The *in vivo* function of PDGF signaling has been studied with gene targeting experiments (25, 26). PDGF-BB or PDGFRβ knock-out mice die during late gestation from cardiovascular complications (27, 28), suggesting the importance of PDGF-BB/PDGFRβ signaling in the myocardiac development of mice. Although the physiological functions of PDGF-BB/PDGFRβ signaling in myocardiac cells are not fully understood, PDGFRβ is expressed in adult rat heart (29) and rat cardiomyocyte-derived H9c2 cells (30), and PDGF-BB/PDGFRβ signaling also controls the proliferation of neonatal rat cardiomyocytes (31). These reports suggest that the PDGF-BB/PDGFRβ signaling pathway plays an important role in the cellular physiology of myocardiac cells, although the precise regulatory mechanism for the signaling pathway and its relation to cellular redox-dependent regulation are not yet clarified.

In the present study we explored the effect of overexpression of GRX on PDGF-BB-dependent signaling and cell proliferation in myocardiac H9c2 cells. We found that overexpression of GRX suppressed the tyrosine phosphorylation of PDGFRβ after stimulation with PDGF-BB, resulting in a suppression of the PDGF-BB-dependent cell proliferation. Furthermore, we describe a novel regulatory mechanism for PDGF-BB signaling involving the redox-dependent regulation of low molecular weight protein-tyrosine phosphatase (LMW-PTP) by GRX in a GSH-dependent manner.

MATERIALS AND METHODS

Antibodies and Reagents—Rabbit anti-mouse GRX polyclonal antibody was prepared as described before (20). Rabbit antibodies against PDGFRβ and phospho-(Tyr-751)-PDGFRβ were obtained from Cell Signaling Technology. Mouse anti-glyceraldehyde-3-phosphate dehydrogenase monoclonal antibody and protein-tyrosine phosphatase inhibitor III (PTPI-III; α-bromo-4-(carboxymethoxy)-acetophenone) were from Chemicon (Temecula, CA). Sheep anti-LMW-PTP polyclonal antibody for immunoprecipitation was from Exalpha Biologicals (Watertown, MA). Rabbit anti-Myc tag polyclonal antibody was purchased from Upstate Biotechnology. Anti-c-Myc monoclonal antibody-conjugated agarose beads were obtained from BD Biosciences Clontech. ^{125}I-Labeled PDGF-BB (25 μCi/ml) was purchased from Amersham Biosciences. 4-Acet-

amido-4'-maleimidylstilbene-2,2'-disulfonic acid (AMS) was purchased from Molecular Probes. PDGF-BB, GSH, GSSG, NADPH, 3-(4,5-dimethyl-thiazole-2-yl)-2,5-diphenyl tetrazolium bromide (MTT), *p*-nitrophenyl phosphate, and mouse anti-FLAG monoclonal antibody were from Sigma. GSSG reductase was from Roche Applied Science. H_2O_2, $CdCl_2$, and dithiothreitol (DTT) were from Wako Pure Chemicals (Osaka, Japan).

Cell Line and Culture—H9c2 cells, a clonal line derived from embryonic rat heart, were obtained from American Type Culture Collection (CRL-1446). H9c2 cells which had been transfected with the expression vector for mouse GRX1 cDNA have been described previously (20). Cell lines (GRX22 and -30) expressing high levels of FLAG-tagged GRX protein were used in the study. H9c2 cells and gene-transfected cells were cultured in Dulbecco's modified Eagle's medium supplemented with 10% fetal calf serum (FCS) containing 75 μg/ml G418 and 75 μg/ml hygromycin B in a humidified atmosphere of 95% air and 5% CO_2 at 37 °C.

Cell Proliferation—The proliferation of cultured cells was evaluated by measuring attached live cells photometrically after staining with crystal violet. The cells (5000) were placed in 100 μl of medium/well in 96-well plates and cultured in medium containing 0.5% FCS with or without 0.5 nM PDGF-BB for specific periods. Then the cells were fixed with 4% paraformaldehyde in phosphate-buffered saline (pH 7.5), washed, and stained with 0.01% crystal violet at room temperature for 20 min. Each well was extensively washed with water and dried. The stained cells were lysed by adding 100 μl of lysis buffer A (10% SDS and 0.1 N HCl), and the cell number was then estimated photometrically by measuring the absorbance at 570 nm using a microplate reader.

Immunoblot Analysis—Cultured cells were harvested and lysed for 20 min at 4 °C in lysis buffer B (20 mM Tris (pH 7.2), 150 mM NaCl, and 1% Nonidet P-40, including protease inhibitors (20 μM phenylmethylsulfonyl fluoride, 50 μM pepstatin, and 50 μM leupeptin)). The protein concentration was determined using a BCA assay kit (Pierce). Protein samples were electrophoresed on SDS-polyacrylamide gels (7.5–15%) under reducing conditions as described previously (32). The proteins in the gels were transferred onto a nitrocellulose membrane. The membranes were blocked in Tris-buffered saline (TBS, 10 mM Tris-HCl (pH 7.5) and 150 mM NaCl) containing 0.1% (v/v) Tween 20 (TBST) and 5% (w/v) nonfat dry milk and then reacted with primary antibodies in TBST containing 5% (w/v) bovine serum albumin or 5% (w/v) nonfat dry milk overnight with constant agitation at 4 °C. After several washes with TBST, the membranes were incubated with peroxidase-conjugated secondary antibodies. Proteins in the membranes were then visualized using the enhanced chemiluminescence (ECL) detection kit (Amersham Biosciences) according to the manufacturer's instructions.

Immunoprecipitation—Cultured cells were harvested and lysed in lysis buffer B. Cell lysates normalized for protein levels were immunoprecipitated using anti-c-Myc monoclonal antibody-conjugated agarose beads for 2 h at 4 °C. The beads were washed three times with cold lysis buffer B. For the immunoblot analysis, the beads were resuspended in 100 μl of SDS sample

buffer containing DTT and boiled for 3 min. Then the supernatant was directly subjected to SDS-PAGE as described above.

Reverse Transcription-PCR—Total RNA was prepared from cultured cells using the standard protocol and was reverse-transcribed using a One Step RNA PCR kit (avian myoblastosis virus (AMV)) (TaKaRa Biomedicals, Japan) with AMV-derived reverse transcriptase XL according to the manufacturer's instructions. PCR was run for 25 cycles of 95 °C for 0.5 min at 65 °C and for 0.5 min at 72 °C for 1.5 min. Primer sequences were as follows: for rat LMW-PTP (33) (GenBank[TM] accession number NM_021262), forward, 5'-CAT GGC AGA GGT TGG GTC CAA GTC AGT GC-3', and reverse, 5'-GCT AGT GAG TCT TCT CCA GGA AGG CCT TG-3'; for rat GRX (GenBank[TM] accession number NM_022278), forward, 5'-CGG CAT GGC TCA AGA GTT TGT GAA CTG CAA AAT CC-3', and reverse, 5'-GTG GTT ACT GCA GAG CTC CAA TCT GCT TTA GCC GC-3'; for rat β-actin (GenBank[TM] accession number BC063166), forward, 5'-GAG CTA TGA GCT GCC TGA CG-3', and reverse, 5'-AGC ATT TGC GGT GCA CGA TG-3'.

Construction of LMW-PTP Gene Expression Vector—Full-length human LMW-PTP cDNA was cloned from total RNA of human colon cancer HCT8 cells by reverse transcription-PCR using Super Script II RNase H reverse transcriptase (Invitrogen) and Advantage HF2 Taq polymerase (BD Biosciences Clontech) with the following primer pair, which was designed on the basis of reported nucleotide sequences for human LMW-PTP (34) (GenBank[TM] accession number M83653): forward, 5'-CGT GGA TCC GAG AAG ATG GCG-3', and reverse, 5'-CCC GAA TTC TCA GTG GGC CTT-3'. The amplified DNA fragments were subcloned into a TA cloning vector (pCRII, Invitrogen), and the nucleotide sequences were confirmed by sequencing with an ALFexpress II system (Amersham Biosciences). The LMW-PTP cDNA was cloned into a C-terminal Myc-tagged expression vector, pcDNA3.1/Myc-His (Invitrogen) under the control of the CMV promoter for expression in mammalian cells and also was cloned into a bacterial expression vector, pGEX6p-1 (Amersham Biosciences). The gene transfection into mammalian cells was performed using Lipofectamine Plus reagent (Invitrogen) according to the manufacturer's directions.

RNA Interference and Transfections—Double-stranded small interfering RNAs (siRNAs) corresponding to rat GRX DNA sequences (GenBank[TM] accession number NM_022278) (5'-ACU GCA AGA UUC AGU CUG GdTdT-3' (siRNA-GRX-1) and 5'-AAC GUG GUC UCC UGG AAU UdTdT-3' (siRNA-GRX-2)) and to rat LMW-PTP DNA sequences (GenBank[TM] accession number NM_021262) (5'-CAC AUU GCA CGG CAG AUU AdTdT-3' (siRNA-LMW-PTP-1) and 5'-UGA GAG AUC UGA AUA GAA AdTdT-3' (siRNA-LMW-PTP-2)) were synthesized and annealed by Samchully Pharmaceuticals, Seoul, Korea. siRNAs were transfected into the cells using Lipofectamine2000 (Invitrogen) according to the manufacturer's protocol with a final siRNA concentration of 100 nM.

LMW-PTP Activity Assay—The activity of LMW-PTP was measured according to the methods of Chiarugi *et al.* (35) with a slight modification. Briefly, the LMW-PTP expression vector was transfected into control and GRX gene-transfected H9c2 cells. After 24 h of transfection, the cells were lysed, and the cell

lysates normalized for protein levels were subjected to immunoprecipitation using anti-c-Myc monoclonal antibody-conjugated agarose beads at 4 °C for 2 h. In each experimental condition, duplicate immunoprecipitates were prepared and subjected to the PTP activity assay or to immunoblot analysis for estimation of the level of LMW-PTP obtained in each immunoprecipitation. After washing, the beads were incubated at 37 °C for 30 min in 0.1 M sodium acetate (pH 5.5), 1 mM EDTA, and 4 mM p-nitrophenyl phosphate, then the reaction was stopped by the addition of 6 N NaOH. Aliquots of the mixture were used to determine the phosphatase activity spectrophotometrically by measuring the absorbance at 410 nm. Each activity was standardized by comparing with the level of LMW-PTP in the immunoprecipitates densitometrically estimated in immunoblot analysis and expressed as the relative value to the activity for the untreated control (% of untreated control). Furthermore, LMW-PTP activity *in vitro* was also measured for recombinant LMW-PTP after incubation with or without H_2O_2. The aliquots were diluted 20-fold by adding 0.1 M sodium acetate (pH 5.5), 1 mM EDTA and subjected to the PTP activity assay as described above. Activity was quantified by comparison with a standard curve (0.01–0.2 mM p-nitrophenol).

Purification of Recombinant LMW-PTP and Generation of Antibody against LMW-PTP—LMW-PTP was purified with the glutathione S-transferase (GST) gene fusion system (Amersham Biosciences) according to the manufacturer's instructions. In brief, *E. coli* strain BL21 cells were transformed with pGEX6p-LMW-PTP, and protein expression was induced by isopropyl β-D-1-thiogalactopyranoside. GST-fused LMW-PTP (GST-LMW-PTP) was affinity-purified from cell lysates using glutathione-Sepharose 4B (Amersham Biosciences) and then digested with PreScission protease. The cleaved GST was removed from glutathione-Sepharose 4B, and LMW-PTP was purified. The LMW-PTP was used to immunize rabbits to generate anti-LMW-PTP antibodies and also used for *in vitro* experiments concerning redox regulation of LMW-PTP as described below.

Determination of the Redox State of LMW-PTP in Vitro—The redox state of LMW-PTP was assessed by modifying free thiol with AMS (20). Briefly, recombinant LMW-PTP (2 μg) was reduced by incubation with 50 mM DTT for 30 min on ice. DTT was then removed by gel filtration on NAP-10 columns (Amersham Biosciences). Reduced LMW-PTP was incubated at room temperature for the periods indicated with H_2O_2 in buffer with or without the GRX (4–40 μg) and/or GSH-regenerating system as described (20). The GSH-regenerating system was composed of GSH/GSSG (1 mM GSH and 0.05 mM GSSG), NADPH (1 mM), and GSSG reductase (GR) (1.2 units). After incubation, LMW-PTP protein was incubated with buffer containing a final concentration of 50 mM Tris-HCl (pH 7.4), 1% SDS, and 15 mM AMS at 4 °C for 1 h. The reaction was stopped by the addition of 5× SDS sample buffer. Proteins were separated by 15% SDS-PAGE with or without DTT and blotted to a nitrocellulose membrane. Proteins in the membrane were then visualized by immunoblot analysis as described above.

Peroxide Quantification—Peroxide was quantified using the PeroXOquant quantitative peroxide assay kit (Pierce) according to the manufacturer's instructions. In brief, cells were incu-

bated with PDGF-BB for given periods. Cells were then harvested and lysed on ice in 100 μl of distilled water by sonication using an ultrasonic applicator (Bioruptor UCD-200T, COSMO BIO, Tokyo, Japan). Working reagent (100 μl) was mixed with 10 μl of lysate and incubated at room temperature for 15–20 min. The purple product composed of Fe^{3+}-xylenol orange complex was detected spectrophotometrically at 570 nm in the reaction mixture. Activity was quantified by comparison with a standard curve (1–50 μM H_2O_2). The protein concentration was determined using a BCA assay kit (Pierce).

Statistical Analysis—Statistical analysis was performed using Student's t test or analysis of variance (StatView software). Significance was set at $p < 0.05$.

RESULTS

Overexpression of the GRX Gene Inhibits PDGF-induced Proliferation of H9c2 Cells—Rat myocardiac H9c2 cells were transfected with mouse GRX1 gene expression vectors to obtain two cell lines overexpressing GRX. Fig. 1A shows that expression of GRX increased in the overexpressors (GRX22 and GRX30) and was immunologically undetectable in mock-transfected (control) H9c2 cells. Recently it has been reported that an antioxidant inhibited cell growth by blocking the phosphorylation of tyrosines in PDGFRβ elicited by PDGF-BB (36). In H9c2 cells PDGF-BB induces cell proliferation through PDGFRβ (30). We also examined the PDGF-BB-dependent proliferation of H9c2 cells in culture medium containing 0.5% FCS with different concentrations of PDGF-BB (0–0.5 nM) and found that the cells proliferated with PDGF-BB in a dose-dependent manner (Fig. 1B, inset). The result showed that 0.5 nM PDGF-BB could sufficiently stimulate the proliferation of H9c2 cells and was consistent with a previous report by Brostrom *et al.* (30). To investigate the functional role of overexpressed GRX in myocardiac cell proliferation, control and GRX gene-transfected cells were cultured in medium supplemented with 0.5% FCS with or without 0.5 nM PDGF-BB, then cell proliferation was analyzed as described under "Materials and Methods." In Fig. 1B, after 3 days of culture with 0.5 nM PDGF-BB, the cell count had doubled in control cells, but the increase was suppressed among the transfectants. On the other hand, without PDGF-BB, proliferation was apparently suppressed in all cells. To investigate whether PDGF-BB signaling is influenced by overexpression of GRX, the phosphorylation status of PDGFRβ was examined immunologically in the cells treated with 0.5 nM PDGF-BB (Fig. 1C). In control cells phosphorylation of PDGFRβ was markedly increased by PDGF-BB, but the increase was apparently suppressed in GRX gene-transfected cells treated with PDGF-BB. Together, these results indicate that PDGF-dependent cell proliferation was suppressed by overexpression of GRX in H9c2 cells through the suppressed phosphorylation of a specific receptor, PDGFRβ. Using ^{125}I-labeled PDGF-BB, the binding of PDGF-BB both to control and GRX gene-transfected cells was investigated as described in the supplemental material. The results showed that overexpression of GRX did not influence the PDGF-BB binding to the cells (supplemental Fig. S1, A and B). Furthermore, we examined cell surface expression of PDGFRβ in control and GRX gene-transfected cells after biotinylation of cell surface proteins and found that overex-
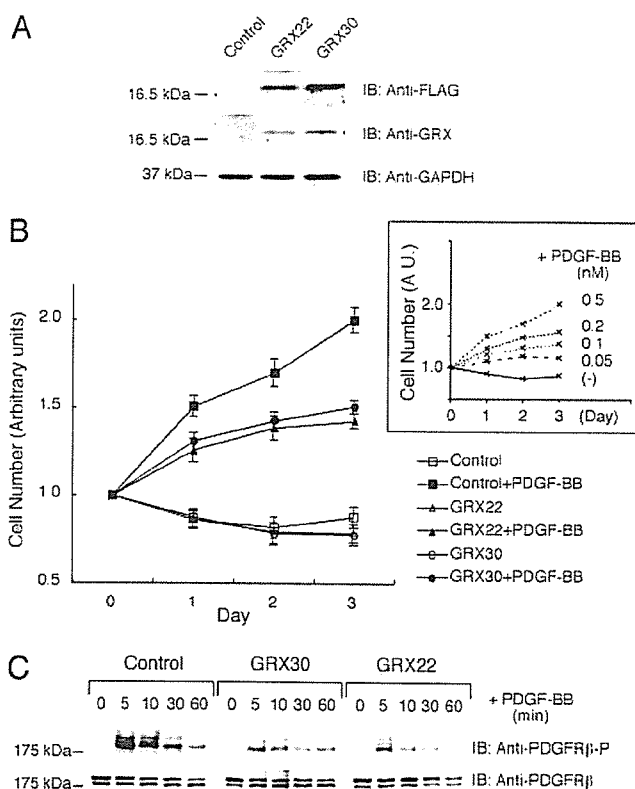

FIGURE 1. **Overexpression of GRX suppresses the PDGF-dependent cell growth.** A, expression of GRX in mock-transfected (*control*) and GRX gene-transfected (*GRX22* and *GRX30*) H9c2 cells. The expression levels of proteins were estimated by immunoblot (*IB*) analysis using antibodies against GRX (rabbit polyclonal) and FLAG (mouse monoclonal) as described under "Materials and Methods." Mouse anti-glyceraldehyde-3-phosphate dehydrogenase monoclonal antibody was used for the loading controls. B, proliferation of control and gene-transfected H9c2 cells cultured for 3 days in medium containing 0.5% FCS with or without PDGF-BB (0.5 nM). Cell proliferation was evaluated by measuring attached live cells photometrically after staining with crystal violet as described under "Materials and Methods." Dose-dependent proliferation with PDGF-BB is shown in control cells cultured in the medium containing 0.5% FCS with or without PDGF-BB (0–0.5 nM) (*inset*). Each value represents the mean of four independent experiments, and the S.D. was always within 10% of the mean. *A.U.*, absorbance units. C, time course of phosphorylation of PDGFRβ in control and gene-transfected H9c2 cells stimulated with PDGF-BB. Cells were treated with 0.5 nM PDGF-BB for the period indicated. Phosphorylation of PDGFRβ was estimated by immunoblot analysis using rabbit antibodies against PDGFRβ and phospho-(Tyr-751)-PDGFRβ. The data represent three independent experiments.

pression of GRX did not change the expression level of cell surface PDGFRβ (supplemental Fig. S1C). Together, these results indicate that overexpression of GRX does not influence the ligand-receptor binding mechanism of PDGF-BB in H9c2 cells.

LMW-PTP Regulates Phosphorylation of PDGFRβ—For the dephosphorylation of PDGFR, there are various PTPs reported, which include Src homology 2-containing protein-tyrosine phosphatase (SHP)-1 and SHP-2, density-enhanced protein-tyrosine phosphatase-1 (DEP-1), PTP-1B, PTP-PEST, T-cell protein-tyrosine phosphatase (TC-PTP), and LMW-PTP (37, 38). Among them, we focused on LMW-PTP because its redox-dependent regulation was extensively studied in the case of PDGF-BB signaling (39). We examined the expression of LMW-PTP in H9c2 cells by reverse transcription-PCR and immunoprecipitation followed by immunoblotting using anti-LMW-PTP antibodies as described in the supplemental material. The
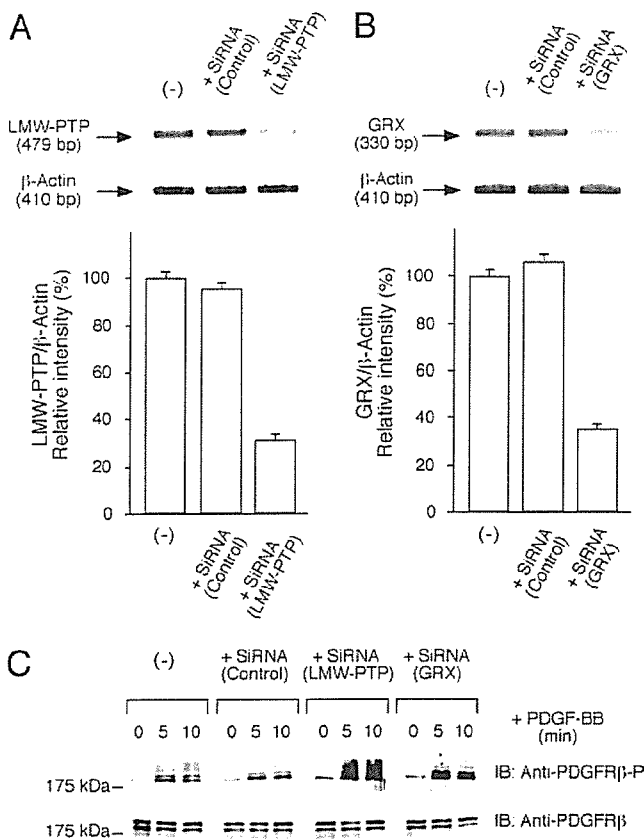
FIGURE 2. **Transfection of siRNAs for LMW-PTP and GRX up-regulates the phosphorylation of PDGFRβ in H9c2 cells treated with PDGF-BB.** To down-regulate the expression of LMW-PTP (A) and GRX (B), specific siRNAs (100 nM) for LMW-PTP and GRX were designed for each gene and transfected into H9c2 cells as described under "Materials and Methods." After 48 h transfection the cells were lysed, and PCR analysis was performed to evaluate the transcriptional expressions of LMW-PTP (A) and GRX (B). siRNAs bearing scramble sequences were also transfected into the cells as controls. The expression of β-actin was also shown as a control. Each value represents the mean ± S.D. of three independent experiments. C, after 48 h transfection with siRNAs, cells were serum-starved for 24 h and then stimulated with 0.5 nM PDGF-BB for the periods indicated. The phosphorylation status of PDGFRβ was examined by immunoblot (IB) analysis using rabbit antibodies against PDGFRβ and phospho (Tyr-751)-PDGFRβ. The data represent three independent experiments.

results showed that the levels for LMW-PTP were similar in control and GRX gene-transfected cells, indicating that LMW-PTP is expressed in H9c2 cells, and the expression level is not influenced by overexpression of the GRX gene (supplemental Fig. S2). To investigate whether LMW-PTP is responsible for the dephosphorylation of PDGFRβ in H9c2 cells, LMW-PTP expression was down-regulated by siRNA transfection, and the effect of suppressed LMW-PTP expression on PDGF signaling was examined. Cells were transfected with siRNAs for LMW-PTP for 48 h, then the transcriptional level of LMW-PTP was examined by reverse transcription-PCR as described under "Materials and Methods." As shown in Fig. 2A, the expression of LMW-PTP was apparently suppressed in cells transfected with siRNAs compared with cells transfected with or without control siRNA bearing scramble sequences for LMW-PTP. After transfection with siRNA, cells underexpressing LMW-PTP were treated with PDGF-BB, and the level of tyrosine phosphorylation of PDGFRβ was examined in immunoblot analysis

(Fig. 2C). The result showed that the level of phosphorylation was apparently increased in cells transfected with siRNAs for LMW-PTP compared with controls. Together, these results demonstrate that LMW-PTP is an endogenous PTP responsible for the dephosphorylation of PDGFRβ in H9c2 cells.

Next, to investigate whether GRX affects the dephosphorylation of PDGFRβ in H9c2 cells, the expression of GRX was down-regulated by siRNA transfection, and the effect of suppressed GRX expression on PDGF signaling was examined. Cells were transfected with siRNAs targeting GRX for 48 h, then the transcriptional level of GRX was examined by reverse transcription-PCR as described under "Materials and Methods." As shown in Fig. 2B, the expression of GRX was apparently suppressed in cells transfected with siRNAs compared with cells transfected with or without control siRNA. After transfection with siRNA, cells underexpressing GRX were treated with PDGF-BB, and the level of tyrosine phosphorylation of PDGFRβ was examined in immunoblot analysis (Fig. 2C). The result showed that the level of phosphorylation was apparently increased in cells transfected with siRNAs for GRX compared with controls. Together, these results demonstrate that the expression of GRX negatively regulates PDGF signaling to suppress the phosphorylation of PDGFRβ in H9c2 cells treated with PDGF-BB.

To further examine the involvement of LMW-PTP in the mechanism regulating PFGF-BB signaling, we prepared the cells transiently transfected with the expression vector for LMW-PTP, because the endogenous level of LMW-PTP protein in H9c2 cells was too low to investigate its biochemical characteristics. To clarify whether LMW-PTP regulates the phosphorylation of PDGFRβ in H9c2 cells, the level of tyrosine phosphorylation of PDGFRβ was examined in an immunoblot analysis using H9c2 cells transfected with two amounts of LMW-PTP gene expression vector, pcDNA-LMW-PTP. As shown in Fig. 3A, the level of phosphotyrosine in PDGFRβ was decreased by transfection with pcDNA-LMW-PTP. To investigate whether transient expression of LMW-PTP gene influences the expression level of cell surface PDGFRβ, we immunoprecipitated PDGFRβ from cell lysates of the cells transfected with or without pcDNA-LMW-PTP after biotinylation of cell surface proteins, and immunoprecipitates were examined by immunoblot analysis to detect PDGFRβ or biotinylated proteins. The results showed that the expression of exogenous LMW-PTP does not change the expression level of cell surface PDGFRβ (data not shown). To confirm that the decrease in the tyrosine phosphorylation of PDGFRβ was due to an increase in LMW-PTP activity caused by the gene transfection, the effect of PTP inhibitor III (PTPI-III) on the phosphorylation status of PDGFRβ was examined in the cells transfected with pcDNA-LMW-PTP. PTPI-III is a cell-permeable broad-range inhibitor of PTPs (40). In Fig. 3B, *upper*, the cells transfected with pcDNA-LMW-PTP were pretreated with various concentrations of PTPI-III for 30 min. Expressed Myc-tagged LMW-PTP was immunoprecipitated, then the activity for LMW-PTP was assayed in the immunoprecipitates as described under "Materials and Methods." The LMW-PTP activity was decreased by PTPI-III in a dose-dependent manner. In Fig. 3B, *lower*, the status of PDGFRβ was also examined by
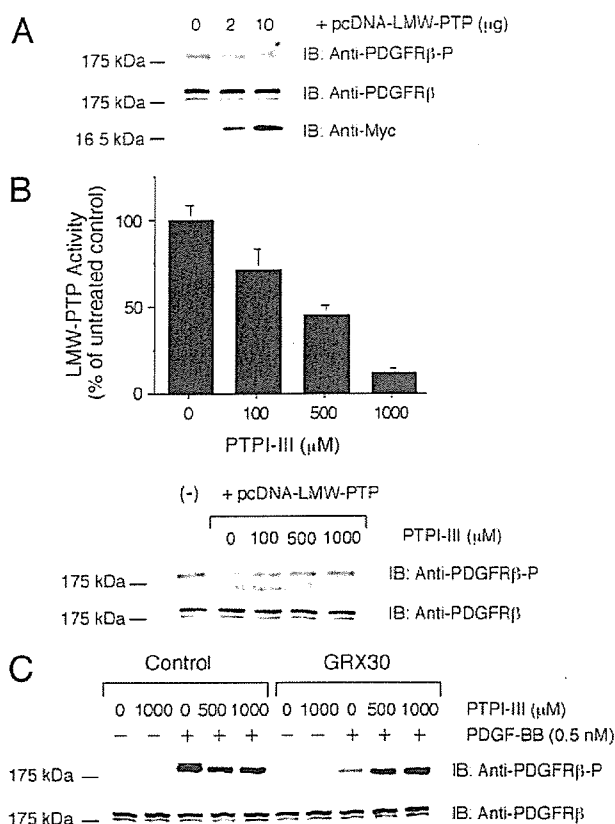
A

B

C

FIGURE 3. Overexpression of LMW-PTP decreases the phosphorylation of PDGFRβ through the phosphotyrosine phosphatase activity. *A,* H9c2 cells were transfected with various concentrations of LMW-PTP expression vector (pcDNA-LMW-PTP) as described under "Materials and Methods." After 24 h the level of phosphorylated PDGFRβ was examined by immunoblot (*IB*) analysis using rabbit antibodies against PDGFRβ and phospho-(Tyr-751)-PDGFRβ. The expression of exogenous Myc-tagged LMW-PTP was detected with rabbit anti-Myc polyclonal antibody. The data represent three independent experiments. *B,* after 24 h of transfection with pcDNA-LMW-PTP, H9c2 cells were treated for 30 min with various concentrations of PTPI-III, an inhibitor for PTP. Expressed Myc-tagged LMW-PTP was immunoprecipitated using anti-c-Myc monoclonal antibody-conjugated agarose beads, and then the activity for LMW-PTP was assayed in the immunoprecipitates as described under "Materials and Methods" (*upper*). Each value represents the mean ± S.D. of three independent experiments. The phosphorylation status of PDGFRβ was examined by immunoblot analysis as described above (*lower*). The data represent three independent experiments. *C,* control and GRX gene-transfected H9c2 cells were serum-starved for 24 h, treated with the indicated concentration of PTPI-III for 30 min, and then stimulated with or without 0.5 nM PDGF-BB. The phosphorylation status of PDGFRβ was examined by immunoblot analysis as described above. The data represent three independent experiments.

immunoblot analysis in the LMW-PTP gene-transfected cells treated with PTPI-III. Although the phosphorylation of PDGFRβ was apparently suppressed by transfection with pcDNA-LMW-PTP, the level gradually increased on treatment with PTPI-III in a dose-dependent manner. These results indicate that overexpression of the LMW-PTP gene causes a decrease in the phosphorylation of PDGFRβ simply through increased LMW-PTP activity.

Next, to investigate how endogenous LMW-PTP activity influenced the PDGF-BB-stimulated phosphorylation of PDGFRβ, the status of PDGFRβ was examined in the control and GRX gene-transfected cells treated with or without PDGF-BB and/or various concentrations of PTPI-III. Control

and GRX gene-transfected cells were pretreated with or without PTPI-III for 30 min and then stimulated with PDGF-BB. In Fig. 3*C,* the level of phosphorylated PDGFRβ after stimulation with PDGF-BB was highly increased in control cells compared with GRX gene-transfected cells. This result was consistent with the result shown in Fig. 1*C.* However, when endogenous LMW-PTP activity was suppressed with PTPI-III, the phosphorylation of PDGFRβ was apparently increased in GRX gene-transfected cells treated with PDGF-BB. On the other hand, in control cells treated with PDGF-BB, the phosphorylation level showed no further increase even in the presence of PTPI-III. Thus, phosphorylation levels were similar between control and GRX gene-transfected cells treated with PTPI-III and PDGF-BB. These findings demonstrate that the activity of endogenous PTP such as LMW-PTP plays an important role in the regulation of the phosphorylation status of PDGFRβ in GRX gene-transfected cells treated with PDGF-BB.

The Activity of LMW-PTP Is Up-regulated by Overexpression of GRX—The PTP activity of LMW-PTP is dependent on the level of cellular reduced glutathione (GSH) (35). To know the effect of overexpression of GRX on LMW-PTP, the activity of LMW-PTP was examined in control and GRX-overexpressing cells after transfection with the LMW-PTP gene expression vector. Control and GRX-overexpressing cells were transiently transfected with pcDNA-LMW-PTP. After 24 h of transfection, the cells were treated with PDGF-BB for given periods, and the activity of LMW-PTP was estimated as described under "Materials and Methods." As shown in Fig. 4*A,* the activity was always stronger in GRX-overexpressing cells than controls during the treatment with PDGF-BB, indicating that the expression level of GRX affected the activity of LMW-PTP. To investigate whether the up-regulation of LMW-PTP activity was due to the effect of overexpressed GRX, the effect of cadmium (CdCl$_2$), an inhibitor for GRX (41), on the LMW-PTP activity was examined in control and GRX-overexpressing cells transiently transfected with pcDNA-LMW-PTP. After 24 h of transfection, the cells were treated with or without PDGF-BB and/or CdCl$_2$. Then the activity of LMW-PTP was estimated as described under "Materials and Methods." Treatment with 200 μM CdCl$_2$ reduced the thiol transferase activity of GRX by more than 60% in GRX-overexpressing H9c2 cells (20). As shown in Fig. 4*B,* the LMW-PTP activity was significantly suppressed by CdCl$_2$ in control and GRX-overexpressing cells with or without PDGF-BB, indicating that GRX activity contributed to the activation of LMW-PTP. In Fig. 4*C,* the effect of CdCl$_2$ on the phosphorylation of PDGFRβ was examined in control and GRX-overexpressing cells treated with PDGF-BB. The results showed that the phosphorylation was apparently increased by CdCl$_2$ in control and GRX-overexpressing cells treated with PDGF-BB. The phosphorylation levels were similarly increased in control and GRX-overexpressing cells treated with PDGF-BB. Collectively, these results indicate that the activity for LMW-PTP is up-regulated by overexpression of GRX through the increased thiol transferase activity of GRX. This also suggests that GRX plays an important role in regulating the redox state of LMW-PTP under PDGF-BB treatment.
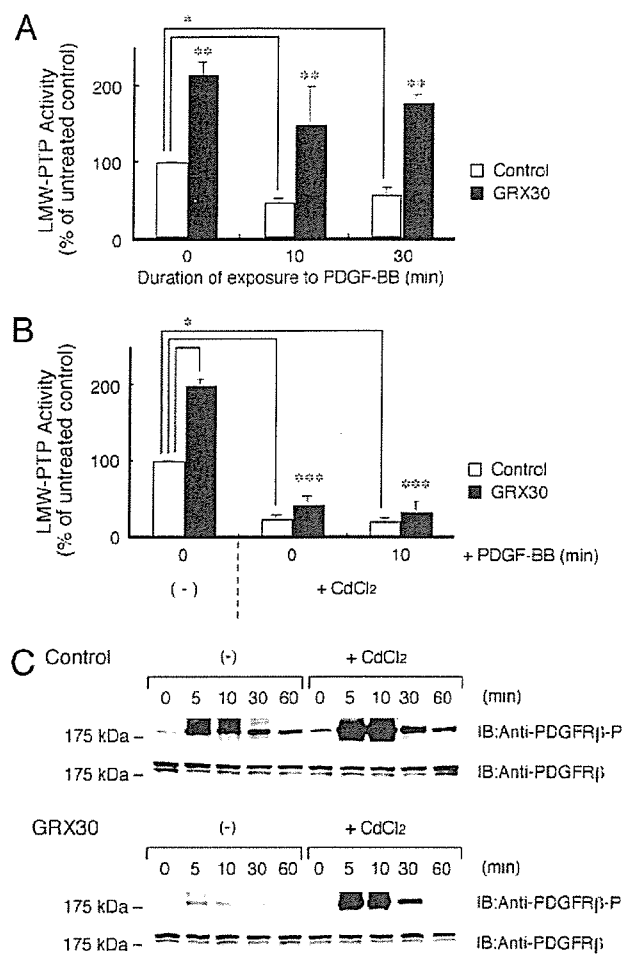
FIGURE 4. **Cadmium diminished the activity of LMW-PTP during PDGF-BB treatment.** A, expression vectors for Myc-tagged LMW-PTP were transiently transfected into control and GRX gene-transfected cells as described under "Materials and Methods." After 24 h cells were serum-starved for 24 h and then stimulated with 0.5 nM PDGF-BB for the periods indicated. Expressed Myc-tagged LMW-PTP was immunoprecipitated, then the activity for LMW-PTP was assayed in the immunoprecipitates as described under "Materials and Methods." *, $p < 0.05$ versus untreated control cells (time 0). **, $p < 0.05$ versus same time point for control cells. B, cells were transfected with the LMW-PTP expression vectors and serum-starved as in A. Then the cells were pretreated with 200 μM CdCl₂ for 1 h and stimulated with 0.5 nM PDGF-BB for the periods indicated. Expressed Myc-tagged LMW-PTP was immunoprecipitated, and the activity for LMW-PTP was assayed as described above. *, $p < 0.05$ versus untreated control cells (time 0). ***, $p < 0.05$ versus untreated GRX30 cells (time 0). C, control and GRX gene-transfected cells were serum-starved for 24 h. Then the cells were pretreated with 200 μM CdCl₂ for 1 h and stimulated with PDGF-BB for the periods indicated. The phosphorylation status of PDGFRβ was examined by immunoblot analysis (IB) using specific antibodies.

Peroxide Is Involved in the Down-regulation of LMW-PTP Activity during PDGF-BB Signaling—The intracellular generation of reactive oxygen species (ROS) is a pivotal event in growth factor-receptor signaling (42–44). There are several reports showing that the phosphorylation status of growth factor receptors is regulated through redox regulation of specific phosphatases (45). LMW-PTP has eight Cys residues in the structure and is oxidized and inactivated by oxidative stress such as nitric oxide and H_2O_2 with the formation of a disulfide bond between Cys-12 and Cys-17 (46, 47). At first, to investigate whether the treatment with PDGF-BB could generate ROS
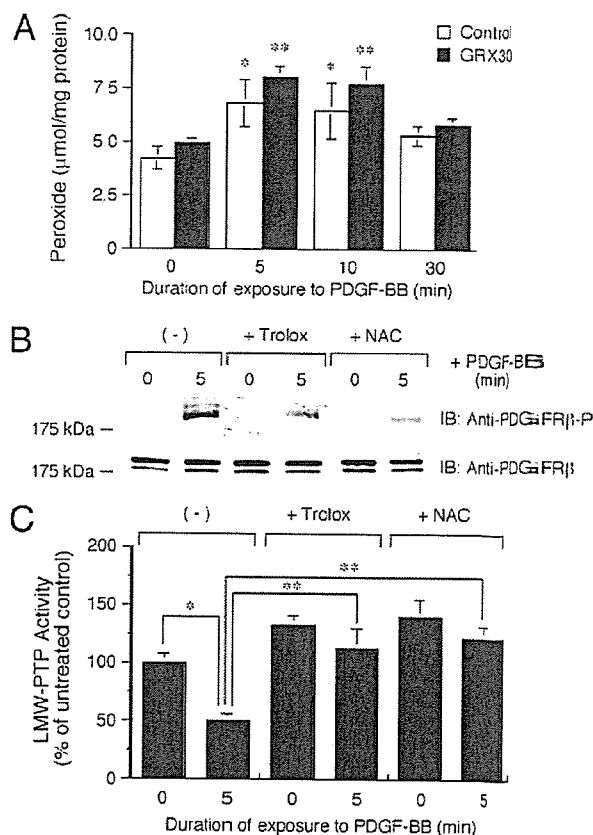

FIGURE 5. **PDGF-BB-induced peroxide production is involved in the phosphorylation of PDGFRβ.** A, control and GRX gene-transfected H9c2 cells were treated with 0.5 nM PDGF-BB for the periods indicated. At each time point cells were harvested, and the intracellular peroxide concentration was measured using a peroxide assay kit (Pierce) as described under "Materials and Methods." Each value represents the mean ± S.D. of three independent experiments. *, $p < 0.05$ versus untreated control cells (time 0). **, $p < 0.05$ versus untreated GRX30 cells (time 0). B, control cells were pretreated with or without 500 μM Trolox (30 min) or 1 mM NAC (30 min) and stimulated with 0.5 nM PDGF-BB for 5 min. The phosphorylation status of PDGFRβ was examined by immunoblot (IB) analysis using specific antibodies. C, control cells were transfected with the LMW-PTP expression vectors and serum-starved as in Fig. 3A. Then the cells were pretreated with or without 500 μM Trolox (30 min) or 1 mM NAC (30 min) and stimulated with 0.5 nM PDGF-BB for 5 min. Expressed Myc-tagged LMW-PTP was immunoprecipitated, then the activity for LMW-PTP was assayed in the immunoprecipitates as described under "Materials and Methods." Each value represents the mean ± S.D. of three independent experiments. *, $p < 0.05$ versus untreated control cells (−) (time 0). **, $p < 0.05$ versus control cells (−) treated with PDGF-BB for 5 m in (time 5).

in the cell, control and GRX-overexpressing cells were treated with PFGF-BB for given periods, and the amount of intracellular peroxide was estimated as described under "Materials and Methods." As shown in Fig. 5A, peroxide assays revealed that the level of cellular H_2O_2 was increased by PDGF-BB with a peak at 5–10 min then decreased to the initial level at 30 min. In this respect, the results suggest that the PDGF-dependent generation of peroxide may lead to the inactivation of LMW-PTP. Next we investigated the effect of chemical antioxidants such as Trolox, an analog of vitamin E, or N-acetyl cysteine (NAC), a supplier of cellular thiols, on the PDGF signaling and LMW-PTP activity. When control and GRX-overexpressing cells were treated with Trolox (500 μM) or NAC (1 mM) for 30 min, production of peroxide almost ceased (data not shown). In Figs. 5, B and C, control cells were transiently transfected with the